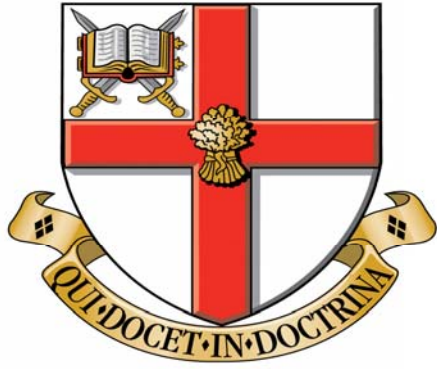


# cdr

## Forecast model for radon concentrations in visitor caves

Item Type	Thesis or dissertation
Authors	Mitchell, Kirsty A.
Publisher	University of Chester
Download date	2026-05-17 11:55:41
Link to Item	<a href="http://hdl.handle.net/10034/297146">http://hdl.handle.net/10034/297146</a>



# University of Chester



**This work has been submitted to ChesterRep – the University of Chester's  
online research repository**

<http://chesterrep.openrepository.com>

Author(s): Kirsty Anna Mitchell

Title: Forecast model for radon concentrations in visitor caves

Date: 20 September 2012

Originally published as: University of Chester MSc dissertation

Example citation: Mitchell, M. A. (2012). *Forecast model for radon concentrations in visitor caves*. (Unpublished master's thesis). University of Chester, United Kingdom.

Version of item: Submitted version

Available at: <http://hdl.handle.net/10034/297146>

MA7091

Forecast Model for Radon Concentrations in  
Visitor Caves

Assesment Number - F14199

K A Mitchell

September 20, 2012

# Contents

<b>1</b>	<b>Introduction</b>	<b>1</b>
<b>2</b>	<b>Literature Review</b>	<b>3</b>
2.1	Dose Calculations . . . . .	5
2.2	Ventilation and Seasonal Variations . . . . .	7
2.3	Radon Flux and Seismic Activity . . . . .	13
2.4	Summary . . . . .	15
<b>3</b>	<b>Datasets</b>	<b>17</b>
<b>4</b>	<b>Data Analysis and Model of Seasonal Radon Concentrations</b>	<b>23</b>
4.1	Moving Averages . . . . .	24
4.2	Curve Fitting . . . . .	25
<b>5</b>	<b>Forecast Model</b>	<b>29</b>
5.1	Construction of the Model . . . . .	29
5.2	Comparison with other Nerja Data . . . . .	32
5.3	Summary . . . . .	34
<b>6</b>	<b>Comparison Against other Datasets</b>	<b>36</b>
<b>7</b>	<b>Discussion</b>	<b>42</b>
<b>8</b>	<b>Conclusions</b>	<b>44</b>
<b>9</b>	<b>Further Work</b>	<b>45</b>
<b>A</b>	<b>Datasets</b>	<b>47</b>
<b>B</b>	<b>Calculations</b>	<b>54</b>
<b>C</b>	<b>Symbols</b>	<b>62</b>



## **Abstract**

The aim of this project is to develop a mathematical forecast model which can be used to forecast the radon concentrations in visitor caves and to assess its validity using statistical analysis of its output and datasets from other caves.

The project consists of a literature review , the creation of a forecast model and a statistical analysis of the results of the model with comparison data. The aim of the literature review is to identify any mathematical models involving radon concentrations and to find any datasets that could be used to develop a forecast model of the seasonal variations in radon concentrations. Having identified a suitable dataset for development of the model a model specific to that cave will be carried out. The results of this model will then be statistically analysed using the original dataset and a second dataset for comparison purposes, following any necessary adjustments.

This will identify whether a forecast model based on observed seasonal variations could be used to predict accurately the radon concentrations in a visitor cave. The use of a second dataset will indicate whether this model has the potential to be applied to other caves or whether predictive models would have to be specifically developed for each cave system.

# Chapter 1

## Introduction

Radon is a naturally occurring radioactive gas which is a product of the uranium-238 decay chain. It is inert, odourless and colourless and can only be detected using a range of specialist equipment. It has a half-life of 3.8 days and emanates from rocks, soil and groundwater in varying concentrations throughout the world depending on location and geology. For instance, certain areas of the UK such as Cornwall and Aberdeen have particularly high radon concentrations due to their geology as they are both granite areas. Radon is also a by product of the nuclear industry, but the amount produced is a tiny fraction compared to the naturally occurring radon.

In the open air radon and its daughter products are dispersed quickly and represent little hazard to the public. However, in buildings and underground structures where ventilation is poor they can build up and reach a level where they may have a detrimental effect on human health. Exposure to high levels of radon has been shown to have the potential to lead to lung cancer or bronchial problems. The health effects to miners from high levels of radon concentrations has been known for some time, but in the 1970's it was realised that other underground formations, such as natural cave systems [25] also had high radon concentration levels, and since then monitoring has been ongoing in a number of caves worldwide. Regulations are in place in the EU (The EURATOM Treaty [8]) for the monitoring and control of radon concentrations in workplaces with respect to dose to workers and the public. One area which falls under the EURATOM regulations are natural caves which are open to the public, resulting in a potential for dose to both visitors and guides. Visitor doses are generally very low, due to very short residence times in caves, but for guides and employees, who spend a considerable length of time in the caves over a year, the annual dose could be significant. In the UK and Action Level of  $400 \text{ Bqm}^{-3}$  (See Appendix D - Glossary for definition) on average for the workplace [15] has been set, compared with

an average outdoor radon concentration of about  $4 \text{ Bqm}^{-3}$  and an average indoor concentration of about  $20 \text{ Bqm}^{-3}$  [21].

The aim of this project is to develop a mathematical model which can be used to forecast the radon concentrations in a visitor cave over a period of time and to assess its validity using a statistical analysis of its output and data sets from other caves for comparison. The level of radon concentration in visitor caves depends on many different factors including the cave structure, number of entrances and natural ventilation points, availability of forced ventilation, position within the cave system, geology, region, the presence of running or dripping water, atmospheric conditions, humidity, and time of year. A model taking all these factors into account would be extremely complex due to the number of influences on the radon concentration [13] and would require a massive amount of monitoring to be carried out to obtain sufficient data. Hence, we will concentrate on the seasonal variations which many of the above issues feed into.

The project consists of a literature review, the creation of a forecast model and a statistical analysis of the results of the model with comparison data. The aim of the literature review is to identify any mathematical models including radon concentrations and to find datasets that can be used to develop a forecast model of the seasonal variations in radon concentrations in visitor caves. Having identified a suitable dataset for development of the model, a forecast model will be developed specific to that cave system. The results of this model will then be statistically analysed using the original dataset.

The model will then be compared to other datasets for comparison purposes, following any necessary changes to, for instance, constants. This will identify whether or not a forecast model based on observed seasonal variations can be used to accurately predict the radon concentrations in a visitor cave. The use of other datasets will indicate whether this model has the potential to be applied to other caves or whether predictive models would need to be specifically developed for each cave system.

# Chapter 2

## Literature Review

The purpose of the literature review is twofold, firstly, to look for and review any mathematical models related to radon concentrations in underground structures, such as visitor caves. Secondly to identify suitable data to use to create a model that could be used to forecast future radon concentrations in a cave system and then try to use this model to predict concentrations in a second cave system with a broadly similar seasonal profile.

The papers included in the review were obtained through the Internet where freely available. The literature on radon is very extensive and for this reason the search for papers is limited to those relating to radon concentrations in underground structures including natural ones such as cave systems, and man-made ones, including mines, tunnels, underground monuments and underground quarries. The papers included in the literature review are listed in Table 2.1 with an indication of the subject areas for each.

The relevant papers fall into three main categories, those whose focus is on the calculation of dose using radon concentrations, those who use the radon concentrations to determine air movement, atmospheric links etc. and those who are interested in radon flux and seismic activity.

Of the papers which are relevant to this study most include data on radon concentrations in air. However, many of these papers present the data in a purely graphical form which cannot be used to create a forecast model. In the remaining papers data has been summarised in a variety of ways from annual averages to monthly averages, over varying lengths of time from two months to a number of years. Although some monitoring has been carried out on a weekly, daily or hourly basis the data from these readings is presented only in graphical form or summarised. For the purpose of this study the data needs to be at least monthly in order to indicate the seasonal changes. This criteria reduces the number of papers with suitable data sets available to five where data is presented in a form which can be used to create a forecast model,

Author	Dose	Ventilation	Seasonal	Seismic
Allodji et al. [1]	•	—	•	—
Cevik et al. [2]	•	—	•	•
Dueñas et al. [4]	•	•	•	•
Dueñas et al. [5]	•	—	•	—
Dueñas et al. [6]	•	•	•	—
Espinosa et al. [7]	•	—	•	—
Garavaglia et al. [9]	—	—	•	•
Géczy et al. [10]	—	•	•	—
Gillmore et al. [11]	•	—	•	—
Grattan et al. [12]	•	—	•	—
Gregorič et al. [13]	—	•	•	—
Hafez et al. [14]	•	—	•	—
Kant et al. [16]	•	—	•	—
Koltai et al. [17]	—	•	—	—
Kowalczk et al. [18]	—	•	•	•
Lario et al. [19]	•	—	•	—
Perrier et al. [22]	•	•	•	—
Perrier et al. [23]	—	•	—	—
Perrier et al. [24]	—	•	•	—
Przylibski et al. [25]	—	•	•	—
Richon et al. [27]	•	•	—	•
Sainz et al. [28]	•	—	—	—
Smetanova et al. [29]	—	•	—	—
Tanahara et al. [30]	—	•	•	—
Tsvetkova et al. [31]	—	—	•	•
Vaupotič et al. [32]	•	—	•	—
Zahorowski et al. [34]	•	•	•	—

Table 2.1: Literature Review papers and their relevant subjects

these are Dueñas et al. (2005) [5], Dueñas et al. (2011) [6], Przylibski (1999) [25], Lario et al. (2005) [19] and Smetanova et al. (2011) [29]. These five data sets and their suitability for this project will be discussed in more detail in the next chapter.

The literature review is split into three sections, dose calculation papers, ventilation and seasonal variation papers, and papers focused on radon emanation from soil (radon flux) and their potential link to seismic activity. A table listing the symbols used in the equations in the literature review and their description is presented in Appendix C.

## 2.1 Dose Calculations

Exposure to radon can cause health effects such as lung cancer and bronchial problems especially where radon has accumulated and reached high concentrations, such as in visitor caves. This was recognised and in 1993 a EURATOM Directive [8] was issued dealing with the risks to workers and the public from high radon concentrations in the workplace. Following on from this the law in many European countries was changed to reflect the recommended levels specified in the Directive.

This project is not concerned with calculating doses to workers or visitors to caves and other underground structures and as a result the papers dealing with dose assessment are reviewed simply from the point of view of the mathematical models used to calculate dose. Discussion on issues such as equilibrium factors, unattached fractions, working limits etc. (See Glossary for definitions) will be noted but not discussed in detail.

Over half of the papers include dose calculations. Of these Dueñas et al. (2011) [6], Dueñas et al. (2005) [5], Dueñas et al. (1999) [4], Espinosa et al. (2008) [7], Sainz et al. (2007) [28], and Zahorowski et al. (1999) [34] give results of dose calculations but do not describe the method and equations used in detail, simply providing references. The remaining papers all describe the methods used to calculate doses. The majority of these are calculations of annual effective dose. One of two methods are used by all but a few authors to calculate the annual effective dose to workers or the public from radon in underground structures, the first is,

$$E = \frac{C_{Rn} \times t}{126,000} \quad (2.1)$$

where E is the effective dose,  $C_{Rn}$  is the radon concentration in  $Bqm^{-3}$  and t is duration of occupation, measured in hours. This equation was developed by Denman and Parkinson (1996) [3] and it assumes an equilibrium

factor (See Appendix D - Glossary for definition) for radon and its progeny of 0.5. In 2000 Qureshi et al. [26] developed an equation which allows for a range of equilibrium factors to be used as well as Dose Conversion Factors (DCF). Their equation calculates the Working Level Month exposure but the majority of the papers present it as seen in equation (2.2). This equation allows for more flexibility and hence a more site specific dose can be calculated.

$$E = \frac{DCF \times C_{Rn} \times F \times t}{3700 \times 170} \quad (2.2)$$

where F is the equilibrium factor for radon and its daughter products.

Lario et al. (2005) includes both methods in his paper and discusses the relative merits of the two, choosing Qureshi's method. This method is also used by Allodji et al. [1], Cevik et al. (2012) [2], Perrier et al. (2004) [22], Kant et al. (2009) [16], Richon et al. (2005) [27] and Vaupotic (2010) [32]. This appears to be the favoured method as only two authors [11] and [12] use the Denman and Parkinson method. The equation appears in a number of forms due to different units being used and the use of PAEC (potential alpha energy concentration), the equation for which which is,

$$PAEC = C_{Rn}xF. \quad (2.3)$$

Cevik [2] also uses soil samples to measure gamma radiation and calculate the total absorbed dose rate, D, in air at 1m above ground level due to the progeny of the radium and thorium decay chains. The formula used is,

$$D = aC_{Ra} + bC_{Th} + cC_K \quad (2.4)$$

where a, b and c are the dose rates per unit activity concentrations of radium, thorium and potassium in  $(Gy h^{-1})/(Bq kg^{-1})$ , and  $C_{Ra}$ ,  $C_{Th}$  and  $C_K$  are the activity concentrations of radium, thorium and potassium.

Three authors include a discussion on the Dose Conversion Factor and unattached fraction (Sainz et al. (2007) [28], Vaupotic (2010) [32] and Zahorowski et al. (1999) [34]) and include equations to calculate an appropriate DCF or unattached fraction for their particular measurements, but as noted earlier this is not central to this study and will not be discussed further here.

Three papers deal with calculating dose for workers from an earlier period and the uncertainties associated with those calculations. In Allodji et al. [1] the doses to French uranium miners are assessed for a series of periods from 1946-1999 overall. Annual exposure to radon and its daughter products were calculated for the period 1956-1982, from measurements of radon made at the time, using equation (2.2). They are then converted into Working Level

Months giving a range from 21.3 for the earliest period to 0.4 for the last period. The remainder of the paper is devoted to identifying and quantifying the uncertainties associated with the assessed doses.

Hafez et al. (2001) [14] and Grattan et al. [12] both attempt to assess the dose from radon to ancient underground workers, Hafez in the tombs of the Valley of the Kings and Grattan in ore mines in the Jordanian Desert, by using modern day radon measurements. Hafez calculates doses to modern day tourists and guides in the tombs as well as the ancient tomb workers using the equation at (2.2) method. The doses to guides and tourists were both within the current guidelines but the doses to ancient workers were within action levels. The equilibrium factor for the tombs is calculated from measurements taken at the site.

Grattan also uses modern measurements to assess the doses to ancient miners in metal ore mines, although there is a modern day aspect to the study too. The orefields still contain a significant quantity of ore and anyone wishing to exploit these mines in the future would need to know if radon abatement would be necessary to protect workers. He uses the equation (2.1) described above. The results of the dose assessment were lower than expected but it is noted that the measurements were taken in Winter and that the Summer concentrations may be significantly higher. It is concluded that if the mines were to be re-activated then radon abatement measures would be necessary. Also discussed are the uncertainties associated with predicting doses to ancient workers, for instance the amount of dust generated in the mines and the ventilation at the time.

The modelling of doses is carried out using well established equations which are tailored to the specific site using site specific equilibrium factors, dose conversion factors, occupancy times and radon measurements. Uncertainties associated with the dose calculations are discussed and in one case quantified, but the main aim is to identify whether doses breach the action levels, necessitating remedial measures.

## 2.2 Ventilation and Seasonal Variations

Ventilation is mentioned in the majority of the papers as it is a major factor in the level of radon concentration, as are seasonal variations, not surprisingly as this was one of the selection criteria. Seasonal variations are obvious in many of the graphical representations of data although only a few papers have this as the focus of the paper.

The papers that focus on ventilation are Kowalczk et al. (2010) [18], Dueñas et al. (1999) [4], Perrier et al. (2004) [22], Gregorič et al. (2011)

[13], Géczy et al. (1993), [10], Koltai et al. (2010) [17], Tanahara et al. (1997) [30], Richon et al. (2005) [27], Perrier et al. (2004) [23], and Perrier et al. (2004) [24]. Seven of these authors include equations or models of either air exchange analysis, ventilation flow rate or radon concentration, however a number of conclusions can be drawn from these papers as a whole concerning radon concentrations in caves, these are;

- Radon is used as a natural tracer of ventilation patterns,
- There is a link between the outside air temperature, ventilation and radon concentration in a cave system,
- The deeper into a cave system you go the higher the radon concentration becomes (with certain exceptions),
- Running water and flooding can have a significant effect on radon concentration and ventilation patterns,
- In most cases ventilation is the most significant factor affecting radon concentration.

[18], [4], [22], [27], [23], and [24] all use radon as a tracer of ventilation patterns which can be used to calculate ventilation flow rate, air exchange analysis or a ventilation index. Radon is a good tracer for ventilation studies because it is found naturally in caves at a higher concentration than in the outside atmosphere due to constant emissions from surfaces, fractures and drip water within the caves [18]. It is a noble gas and is therefore chemically inert and its half life of 2.8 days is generally greater than the rate of turnover of air in caves which is usually around a day. Radon flux (see Section 2.3) is also used in ventilation flow rate calculations, although it is often assumed to be constant for simplicity [22].

The papers listed above, and many others whose focus is not on ventilation per se, establish a link between the outside air temperature and radon concentration. Ventilation is the link between the two. Local weather conditions drive the cave ventilation through outside air temperature and via winds [18]. Differences between air density inside and outside the cave can lead to a density driven flow and as the air density is influenced by temperature the flow between the outside and the cave is closely related to temperature and hence the radon concentration. Outside wind speeds can also affect the air flow between the cave and the outside atmosphere although the effect of this seems to be less than the effect of temperature. The correlation between outside air temperature and radon concentrations was noted in many

of the papers reviewed, even those which did not study the ventilation such as Dueñas et al. (2005) [5].

A number of papers note that radon concentrations are higher further into a cave system or further away from an entrance, for instance [4], [18], [13], and [27] as well as others not focused specifically on ventilation. This is related to the reduction in the level of ventilation deeper in the cave system, however, this cannot be taken as a rule as a number of other factors can have an effect. These include multiple entrances, ventilation points (natural or man-made), variations in radon emanation, fracturing of the surrounding rock and the presence of water. [4] notes that in the Nerja caves the concentrations of radon are highest in the Vestibule, nearest the entrance but this is associated with the high air exchange rate pulling radon into the area and overall the geometric mean increases the further into the cave system the measurements are taken. Another aspect that has an effect on the ventilation and radon concentration is the presence of doors and polymer curtains as discussed in [27] and [23] which change the natural ventilation and hence the radon concentrations.

The presence of water can have a significant effect on the radon concentration in a cave. Cevik et al. (2011) [2] partially attributes the lower winter radon concentrations to the higher water level in the cave due to the some radon being absorbed into the water, lowering the concentration in the cave air. Water, and in particular flooding, can also lead to increased radon concentrations. Kowalczyk et al. (2010) [18] describes flooding events in Hollow Ridge Cave in Florida leading to a ten fold increase in the radon levels partially due to the lack of ventilation.

The level of ventilation at a sampling point, although not the only influence on radon concentration by any means, is the predominant factor affecting the radon concentration in cave air, others include outside-inside temperature differences, wind velocity, atmospheric pressure variations, humidity, karstic geomorphology, porosity and radium content of the the sediment and rocks [6]. The use of radon as a tracer for ventilation systems and the observed effect of ventilation on radon concentrations especially when it is cut off (flooding), or in alcoves where ventilation is minimal demonstrates the link between the two.

Having described the general conclusions of the review of ventilation we will concentrate on the models described in the seven papers which include equations, these are [4], [13], [18], [22], [23], [24], and [27]. All the papers share the same starting point for their calculations which is an equation for the rate of change of radon concentration (mass balance equation), this comes from a paper by Wilkening and Watkins [33] and is as follows,

$$\frac{dC}{dt} = \frac{S}{V}\Phi - \lambda C - \lambda_V(C - C_{ext}) \quad (2.5)$$

where  $C$  is the radon concentration observed in a cavity,  $S$  is the surface area,  $V$  is the volume,  $\Phi$  is the net radon flux at the rock surface,  $\lambda$  is the radon-222 decay constant,  $\lambda_V$  is the ventilation rate and  $C_{ext}$  is the outside radon concentration. The different papers use slightly different symbols for different quantities, for instance Perrier et al. (2004) [22] use  $A$  for radon concentration rather than  $C$ , but the basic equation remains the same. Richon [27] goes on to solve the equation, he states that since the atmospheric radon concentration is negligible compared to the concentration within the cavity the steady state radon concentration in the cavity in the presence of ventilation,  $C$ , is given by;

$$C = \frac{\lambda}{\lambda + \lambda_V} \bar{C} \quad (2.6)$$

where  $\bar{C}$  is the steady state radon concentration without ventilation which is related to the exhalation flux by;

$$\bar{C} = \frac{1}{\lambda} \frac{S}{V} \Phi. \quad (2.7)$$

Using site specific values for  $\Phi$ ,  $\bar{C}$  and  $C$  Richon [27] develops the following equation for calculating the ventilation flow rate.

$$\lambda_V = \lambda \left( \frac{\bar{C}}{C} - 1 \right) \quad (2.8)$$

Perrier et al. (2007) [24], Kowalczyk et al. (2010) [18] and Dueñas et al. (1999) [4] also use the equation to calculate the ventilation flow rate, although the use of different symbols and different assumptions, such as whether the outside radon concentration is assumed to be effectively zero or whether it is assigned a low value and kept in the equation, make the equations look slightly different.

Perrier et al. (2004) [22] also calculates the ventilation flow rate but uses the ratio of Summer to Winter radon concentrations to calculate the volumetric flow rate for an abandoned limestone quarry. He assumes a constant radon flux, a negligible summer ventilation rate and takes atmospheric radon concentration as zero and develops the relation shown in equation (2.9), which is similar to equation (2.8) but using a different ratio. It should be noted that [22] uses  $A$  for radon concentration but for consistency we have used  $C$ .

$$\lambda_V^{winter} = \lambda \left( \frac{C_{summer}}{C_{winter}} - 1 \right) \quad (2.9)$$

where  $\lambda_V^{winter}$  is the winter ventilation flow rate,  $\lambda$  is the radon-222 decay constant as before and  $C_{summer}$  and  $C_{winter}$  are the summer and winter radon concentrations respectively. Having calculated the winter ventilation rate [22] uses it to calculate the volumetric flow rate,  $Q_V$ , as shown in equation (2.10),

$$Q_V = \lambda_V^{winter} V_{tot} \quad (2.10)$$

where  $V_{tot}$  is the total volume of the quarry.

Perrier et al. (2005) [23] applies the equation to a four-box and a five-box ventilation model. The four or five box model means that the cave can be split into section according to where physical barriers are erected, restricting free air exchange, the remaining air exchange between each section can then be analysed using the changes observed in the radon concentrations over time. The four or five simply refers to the number of sections in the tunnel. This is used for the Roseland tunnel in France where the different sections of the tunnel are isolated from each other either by polymer curtains or metal doors, the tunnel is also isolated by an entrance door, therefore having a very different air flow pattern to other cave systems. The use of the four and five box models indicated a change in the number of sections when an additional polymer curtain was installed. The models examine the air exchange between the sections of the tunnel by using the radon concentrations in each section and the differences between adjacent sections. A series of equations for each section are developed to give the rate of change radon concentration with time, assuming a constant radon flux. The purpose of these equations is to use them to examine the radon bursts identified in the tunnel, see Section 2.3.

Gregorič et al. (2011) [13] is the only author who uses the equation to develop a method to calculate radon concentration values. Two of the symbols used have been changed for consistency, these are  $\Phi$  for  $E_{Rn}$ , the radon flux, and  $\lambda_V$  for  $Q$ , the natural ventilation flow rate. Starting from the base mass balance equation (Equation (2.11)) with slight changes,

$$\frac{dC_{cave}}{dt} = \frac{S}{V} \Phi - \lambda C_{cave} - \frac{\lambda_V}{V} (C_{cave} - C_{out}) \quad (2.11)$$

where  $C_{cave}$  is the radon concentration in the cave and  $C_{out}$  is the outside radon concentration. [13] states that due to the complex morphology of the Postojna cave system the natural flow rate and the volume are not known

and, hence, the mass balance equation (Equation (2.11)) can be simplified to,

$$\frac{dC_{cave}}{dt} \approx \Phi - \lambda C_{cave} - \frac{k_i |\Delta T| C_{cave}}{L} \quad (2.12)$$

where  $k_i$  is a constant,  $\Delta T$  is the difference between outside and cave temperatures,  $L$  is distance of the measuring location from the entrance and the outside radon concentration is set at zero as it is so much less than in the cave. The radon flux is calculated by multiplying the radon decay constant by the maximum cave radon concentration, assuming that there is no ventilation and given that values of  $k_i$  can be calculated from measured data for every day using equation (2.13),

$$k_i = \frac{\Phi L}{|\Delta T| C_n} - \frac{\lambda L}{|\Delta T|} - \frac{(C_{n+1} - C_n)L}{dt |\Delta T| C_n} \quad [ms^{-1}K^{-1}] \quad (2.13)$$

where  $C_{n+1}$  and  $C_n$  are average daily radon concentrations for two consecutive days and  $dt$  is 1 day. [13] goes on to calculate two values for  $k_i$ , one for days when the average daily temperature is above  $10^\circ C$  and one for days when the average daily temperature was between  $-6$  and  $10^\circ C$ . On days when the temperature was below  $-6^\circ C$  a constant radon concentration was assumed.

Using the values of  $k_i$  in equation (2.12) predicted radon concentration values are calculated. The results are tested against measured data and gives a correlation coefficient of 0.76 over a two year period, noting that the correlation is poorer in the transitional period of Spring and Autumn. [13] has therefore created a reasonably accurate model for predicting radon concentrations in the Postojna Cave system based on other measured data, such as temperature.

Seasonal variations in radon concentrations are a feature of almost all of the papers in the literature review. The majority demonstrate a typical high in Summer and low in Winter pattern although there are some notable exceptions. The papers dealing with the Roseland Tunnel in France ([23], [27]) do not find any significant seasonal variations as the tunnel is isolated from the outside atmosphere, although they do not rule it out as a factor in the radon concentration levels. Perrier et al. [24] note the significant difference in radon concentrations following heavy rainfall (monsoon) in the Phulchoki Hill Tunnel in Nepal and Lario et al. [19] find that the Altamira Caves in Spain have a radon concentration profile that is opposite to that normally observed, i.e. high in Winter, low in Summer. As the majority of papers find a seasonal variation that is high in Summer and lowest in Winter that is the profile that we shall aim to predict in our forecast model.

## 2.3 Radon Flux and Seismic Activity

Six authors deal with the radon flux (radon emanation from soil, rock, etc.), Cevik et al. (2012) [2], Dueñas et al. (1999) [4], Garavaglia et al. (1998) [9], Kowalczk et al. (2010) [18], Richon et al. (2005) [27] and Tsvetkova et al. (2005) [31]. Three of these ([2], [4], [18]) use the measurements for calculating dose and/or assessing ventilation only. The other three ([9], [27], [31]) focus more on the influences on radon flux and the possible link with local seismicity and crustal deformations, although Richon [27] also examined ventilation and dose.

Cevik [2] uses the measurements from soil samples in two caves in Turkey to calculate the dose from gamma radiation as detailed in Section 2.1, it is noted that there is no strong correlation between the radon concentrations in the cave air and the radium activity concentrations in the soil.

Dueñas (1999) [4] and Kowalczk [18] both measure the radon emanation rate from soil, rock, etc. as part of studies of the ventilation of their respective cave systems. Kowalczk [18] uses the emanation rate of radon in the Marianna Caves in Florida, USA in an air exchange model using radon as a tracer of the caves' natural ventilation. An average emanation rate is calculated and used for simplicity, based on the assumption that the emanation rate is constant. It is noted that this is probably not the case as the measurements are expected to vary temporally and spatially within the cave system.

Dueñas (1999) [4] measures the radon emanation in an accumulation chamber in the Nerja Caves, Spain, and uses it to calculate the radon flux ( $\Phi$ ) (N.B. In the paper the notation  $J_{Rn}$  is used for radon flux, but for consistency  $\Phi$  has been used in this report) using the following equation,

$$\Phi = h \frac{\Delta C_{Rn}}{\Delta t} \quad (2.14)$$

where  $h$  is the height of the accumulation chamber and  $\Delta C_{Rn}$  is the difference between the concentration of the radon inside the accumulation chamber after the accumulation period ( $\Delta t$ ) and the concentration of the radon outside the accumulation chamber. The measurements confirmed that there is a variation in the radon flux between the different halls of the cave system and that the radium content of the rock, soil, etc. is not an important factor in the radon flux for this cave system. The average radon flux was found to be lower than other caves in the area but the data shows coherent behaviour with respect to ventilation of the cave system.

Richon [27] includes dose calculations and ventilation rate calculations which are reviewed in the relevant sections of this report. The equilibrium

concentration of radon from a sample of rock from the cave is measured and this is used to calculate the emanation coefficient  $E_M$  (The paper uses  $E$  for the emanation coefficient but to distinguish it from the effective dose used earlier in this report it has been changed to  $E_M$ ),

$$E_M = \frac{V_c C_{Rn}}{V_s \rho C_{Ra}} \quad (2.15)$$

where  $V_c$  is the volume of the measurement chamber,  $V_s$  is the volume of the sample,  $C_{Rn}$  is the equilibrium concentration of radon,  $C_{Ra}$  is the radium content and  $\rho$  is the rock density. Further measurements are taken in situ at the cave wall surface with an accumulation method, the radon exhalation flux,  $\Phi$ , is calculated from the results using the equation below,

$$\Phi = \frac{V_{cyl} C_{Rn}}{S_{cyl} T_{acc}} \quad (2.16)$$

where  $V_{cyl}$  is the container volume,  $S_{cyl}$  is the container's base surface area,  $C_{Rn}$  is the measured radon concentration and  $T_{acc}$  is the accumulation time. As well as this measured value of the radon flux, it is related back to the emanation coefficient  $E_M$  using the equation shown below for the diffusive exhalation radon flux at the surface of a semi-infinite homogeneous source,

$$\Phi = \lambda E_M \rho C_{Ra} z^* \quad (2.17)$$

where  $\lambda$  is the decay constant of radon,  $\rho$  is the density,  $C_{Ra}$  is the radium content and  $z^*$  is the diffusion length of radon in the rock. The radon flux calculated is then used in the ventilation rate calculations as shown in Section 2.2.

Richon [27] also discusses the influences on radon exhalation flux and in particular their relevance to the transient radon bursts in the radon concentration in cave air observed in the Roseland tunnel, France. The ventilation study demonstrates that the transient bursts are not solely related to changes in natural ventilation, although they are modulated by ventilation, atmospheric pressure variations and radioactive decay. It concludes that they must be caused by transient changes in the radon exhalation flux. The potential influences on the radon exhalation flux are identified as meteorological, hydrogeological and mechanical deformation of the surrounding rock mass. Some hydrogeological work had been carried out but this had not ruled out the influence of hydrogeological effects and more work is recommended to gain a better understanding of all the potential factors and to identify the main contributors. It is noted that if the transient radon bursts are caused

by mechanical deformation of the surrounding rock mass it may be possible to identify a mechanism for analysing earthquake precursors.

Garavaglia [9] measures the radon flux in the Villanova Cave in North-East Italy to study the possibility of using radon emanation from soil in seismic areas as earthquake precursors. Rainfall and barometric pressure are also measured to compare with the radon flux and it is concluded that both rainfall and barometric pressure have an influence on the radon flux in these caves but that the radon response to these influences is non-linear and hence difficult to identify accurately. In addition to this there are periods where the influence of these atmospheric influences disappears, adding to the difficulty. On the issue of using the location for seismic precursor research it concludes that the site is not suitable due to the strong seasonal variations observed and the atmospheric influences discussed above.

Tsvetkova [31] took hourly, daily and monthly measurements of radon in soil air in caves in the Northern Caucasus over a number of years as well as radon concentrations in cave air. The main focus of the paper is the potential for radon emanations being used as earthquake precursors. The data is compared with earthquakes in the region of the caves and further afield, hurricanes and changes in atmospheric parameters. Changes in soil air radon correlate to the three months prior to earthquakes, and very large, repeated spikes (“splashes”) in the hourly radon measurements that are sustained over a period of hours were observed in the  $9 \pm 1$  days prior to an earthquake and before a nearby atmospheric event (hurricane). The radon concentrations in cave air are also compared to earthquakes in the region but no correlation was found as the influence on cave air concentrations of natural ventilation is far greater.

Radon flux is used in the papers for calculating gamma dose, air exchange modelling and to try and predict earthquakes. The first two of these uses are reasonably successful but the use of radon to predict earthquakes is less consistent. In one case the seasonal variations made the site unsuitable as a test site, the other site showed a strong correlation and indicated that there is potential in the use of radon concentrations in soil air to predict earthquakes.

## 2.4 Summary

The first aim of this literature review was to find suitable datasets for analysis and potential use as the basis for a forecast model. Six datasets in five papers were identified and these are discussed in detail in the next chapter. The second aim was to identify and modelling involving radon concentrations. A number of authors used radon concentration measurements to calculate doses

to workers and public, to calculate the levels of radon emanation (flux), and in air exchange analysis (radon mass balance) calculations to identify the ventilation rates, effectively using radon as a natural tracer. Only one of these authors, Gregorič et al. (2011) [13] uses the model to predict radon concentrations in a cave, he uses measurements of radon concentration, temperature and radon flux to calculate temperature related constants that can then be used to find the predicted radon concentration in the cave on any given day relative to a temperature measurement. The method has a reasonable level of success for the cave concerned but is not applied to any other caves it is also based on measured data rather than forecasting radon concentrations based on seasonal variations alone, hence, no models were found that use the forecasting method proposed in this study.

# Chapter 3

## Datasets

A significant issue which must be dealt with before discussing the datasets is the monitoring methods used and the results obtained. A variety of different monitoring regimes and monitoring equipment were used in the various surveys discussed in the literature review. The results would not have initially been produced in  $Bqm^{-3}$ , the units used in this study. However, as  $Bqm^{-3}$  are the standard units for radioactivity all the results, irrespective of initial form, were converted into these units. As a result of this the datasets can be compared directly to each other. The same applies to the monitoring methods, as whichever methods were used, their output, for instance counts per minute, were converted to  $Bqm^{-3}$  and any differences in error margins etc. would have been taken into account at that stage. This allows the datasets to be used as they are without any further adjustments being necessary.

A number of datasets were identified during the literature review. Many can not be used as they only provide seasonal averages over a period of one year. The datasets (See Appendix A) that have potential to be used in the modelling process considered here are:

- Dueñas et al. [5] - Nerja (2005)
- Dueñas et al. [6] - Nerja (2011)
- Przylibski [25] - Niedźwiedzia & Radochowska
- Lario et al. [19] - Altamira
- Smetanova et al. [29] - Domica

All five of the cave systems listed above are natural caves that are open to the public to some extent. They are all situated in Europe, two in Spain, two in Poland and One in Slovakia, and hence there are all in the northern

hemisphere and share the same seasonal pattern. There are no issues with monsoon seasons or other irregular extreme weather events such as hurricanes. Similarly they do not appear to be in areas of high seismic activity like Italy, which can potentially have an effect on radon concentration levels. This means that none of the datasets listed above should be excluded for geographical, atmospheric or geological reasons.

It is important to have at least two sets of data, one to base the model on and another to use as a comparison set. These two sets of data have to have certain similarities in order for them to be used. They must have a similar seasonal profile eg. a peak in the summer months and a trough in the winter and the data must be in the same format, i.e. monthly averages and cover a long enough period of time for the seasonal variation to be obvious.

The Domica dataset gives the monthly mean and median for the radon concentrations measured, however the total period covered is only six months. The data shows promise of following the high summer/low winter profile but the data is insufficient to confirm this, as noted by the author in [29]. For this reason the data is not suitable for the investigation.

The Altamira dataset includes the monthly median, minimum and maximum values for one year. One year may have been sufficient for using to test the model, but the cave has a substantially different seasonal profile (high in winter and low in summer) to the other datasets. This is attributed to higher ventilation rates in [19] but is not discussed in any detail. Because of this different seasonal profile the dataset is not suitable for this study.

The remaining three datasets all provide monthly data and the more usual seasonal variation of high concentrations of radon in Summer and low in Winter. Niedźwiedzia includes multiple sets of results for different parts of the cave for up to two years in duration. Some of the data sets had entries missing where difficulties had been encountered with the measurements, but on the whole this constitutes a comprehensive set of data that could be analysed in a number of different ways.

To assess the consistency of the Niedźwiedzia dataset we calculated the average value for each month in each of the seven halls, see Figure B.1, and carried out a two factor ANOVA without replication to assess the variances. The results are shown in Figure B.2. The results for both the months (rows) and the halls (columns) show that there is a significant difference in means for both factors. The p-value for the months is  $1.50233 \times 10^{-19}$  which is to be expected given the seasonal variation in the radon concentrations for these caves. The p-value for the halls is 0.000381971 which also indicates a significant variation in the mean which is less expected. The reason for this is the variation in the radon concentrations in different areas of the cave system due to ventilation levels and other factors. Given this significant variation

across the dataset it would not be suitable for basing the model on, although it would be a useful dataset to test the model on for comparison purposes.

In the same paper as the Niedźwiedzia dataset is a dataset from a second cave, Radochowska Cave, this provides only fifteen months worth of monthly average concentrations in one position with no gaps which would not be sufficient to base the model on. Nerja (2005) gives monthly averages and maximum and minimum values for one hall in the Nerja Cave complex over a period of one year. Whereas Nerja (2011) gave monthly averages for three different halls in the Nerja Cave complex, each hall covering one of three consecutive years. These three datasets are, therefore, the most promising ones.

The longer the period covered by the dataset the more accurate the forecast model will be, hence, at first sight the Niedźwiedzia dataset would appear to be the optimum choice for the model. However, on closer inspection it can be seen that in Nerja (2011) the three datasets run consecutively giving three years worth of measurements for the same cave system. One concern in using the data in this way is that the three years of data were gathered in three different locations within the cave system. As was discussed previously, the further away from an entrance or ventilation point the measurement is taken the higher the radon concentrations are, although there are exceptions to this in more complex cave systems. In order to assess the impact that this may have on the data the three sets were plotted on the same graph. Their gradients were calculated by differentiating the trendline equation produced by Excel, these are also shown on the graph, see Figure 3.1.

It can be seen from the Figure 3.1 that the three sets of results are reasonably close in terms of monthly averages and the gradients of the lines of best fit using data from the Vestibule and Ballet Halls are within 0.5 of each other and almost parallel. Mirador Hall has a shallower gradient (9.5909) but this simply reflects the slight differences between the seasonal variation from year to year. A two factor ANOVA without replication was carried out on the three sets of radon concentrations from Vestibule, Ballet and Mirador Halls of the Nerja system. The results are shown in Figure 3.2. The p-value for the months (rows) is  $4.68 \times 10^{-15}$  showing that there is significant difference in means between the months for the three halls as would be expected given the seasonal variations. The p-value for the halls (columns) is 0.18 and hence there is no significant difference in the radon concentrations between the three halls.

Overall the three sets of data would appear to give a reasonable basis for creating a three year dataset using them in the time order that the measurements were taken, i. e. Vestibule, Ballet and then Mirador. Ordering the data in this way creates the graph shown in Figure 3.3.

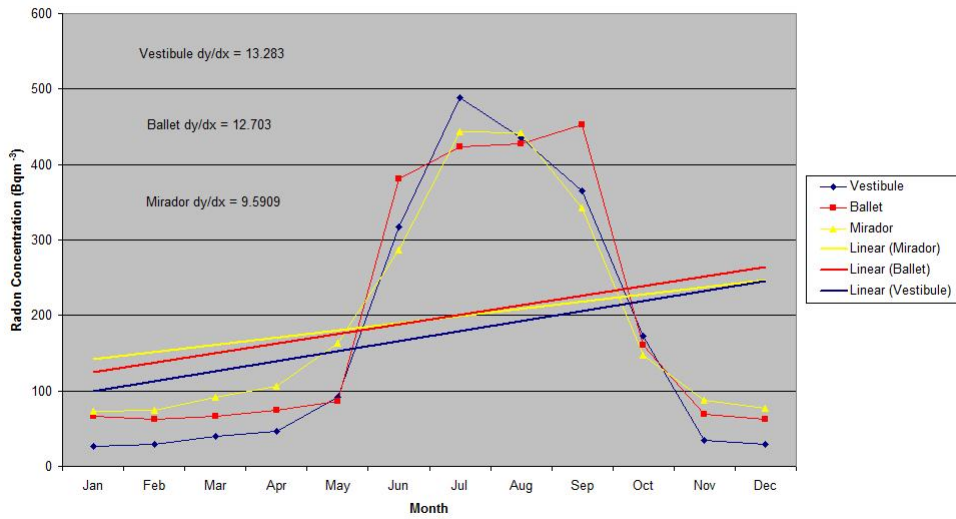


Figure 3.1: Nerja Caves (2011) - Vestibule, Ballet and Mirador

Source of Variation	SS	df	MS	F	P-value	F <sub>crit</sub>
Rows	875048.9722	11	79549.90657	78.96920373	4.67972E-15	2.258518357
Columns	3755.555556	2	1877.777778	1.864070271	0.178713391	3.443356779
Error	22161.77778	22	1007.353535			
Total	900966.3056	35				

Figure 3.2: Nerja Caves (2011) - Vestibule, Ballet and Mirador - Two factor ANOVA without replication

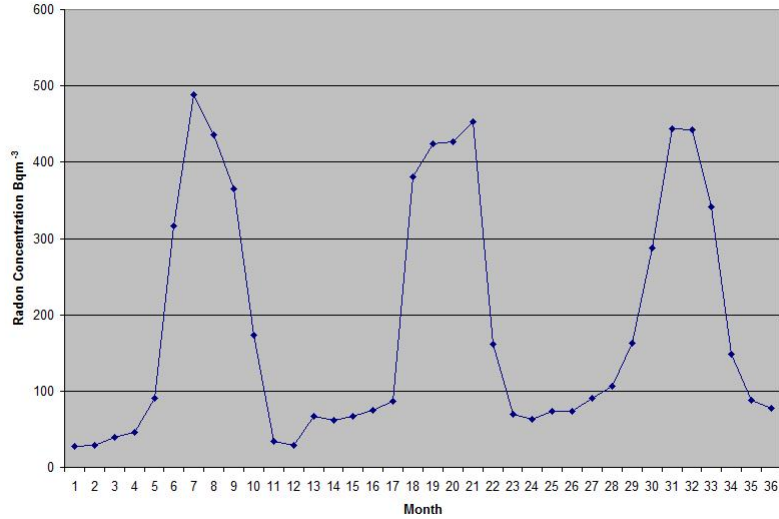


Figure 3.3: Nerja Caves (2011) - Three Year Plot

To assess the appropriateness of using the dataset in this way a multiple regression was carried out on the data, with the radon concentration as the dependent variable and the month and hall as the independent variables values. The results are given in Figure 3.4. The linear regression gives p-values of 0.13 and 0.74 for the month and hall respectively. The coefficients in the regression line are not significant - as would be probably be expected with a dataset of this size.

Given that the Nerja (2011) dataset provides the longest running set of data, that there were no gaps in the data, and noting the reservation that the data came from three different monitoring positions within the cave system, this dataset is chosen to base the model on, with the Nerja (2005) dataset as a potential option for testing and refining the model. The Niedźwiedzia dataset will be used as the comparison dataset.

SUMMARY OUTPUT								
<i>Regression Statistics</i>								
Multiple R	0.264746146							
R Square	0.070090522							
Adjusted R Square	0.013732372							
Standard Error	159.3373691							
Observations	36							
<i>ANOVA</i>								
	<i>df</i>	<i>SS</i>	<i>MS</i>	<i>F</i>	<i>Significance F</i>			
Regression	2	63149.19872	31574.59936	1.243662573	0.301488759			
Residual	33	837817.1068	25388.39718					
Total	35	900966.3056						
	<i>Coefficients</i>	<i>Standard Error</i>	<i>t Stat</i>	<i>P-value</i>	<i>Lower 95%</i>	<i>Upper 95%</i>	<i>Lower 95.0%</i>	<i>Upper 95.0%</i>
Intercept	88.61111111	86.23807299	1.027517291	0.311649974	-86.84156673	264.063789	-86.84156673	264.063789
X Variable 1	11.85897436	7.69288067	1.541551841	0.132718344	-3.792308967	27.51025768	-3.792308967	27.51025768
X Variable 2	10.83333333	32.52460426	0.333081173	0.741179996	-55.33847125	77.00513791	-55.33847125	77.00513791

Figure 3.4: Nerja Caves (2011) - Multiple Regression Results

## Chapter 4

# Data Analysis and Model of Seasonal Radon Concentrations

The first stage of the data analysis will identify the trend within the original data using a range of techniques. These are;

- Semi-averages - this method involves taking the average of the two halves of the data and using these points to create a trendline for the data.
- Moving averages - in this technique the average of a number of periods is taken for each consecutive set of periods and plotted against the central point of the period. If an even number period is used then the first and second set averages are averaged and the result plotted against the midpoint of the two. This will allow us to de-seasonalise the data.
- Trendlines - these will be calculated using Microsoft Excel built in curve fitting facilities to identify the line of best fit against the centred moving average.
- Errors - the difference between the trendlines and the centred moving average (errors) will be calculated and the mean error, mean squared error, absolute mean error and absolute mean squared error will be used to compare the accuracy of each of the trendlines to identify the best fit.

Once the best fit trendline has been identified the construction of the model can proceed.

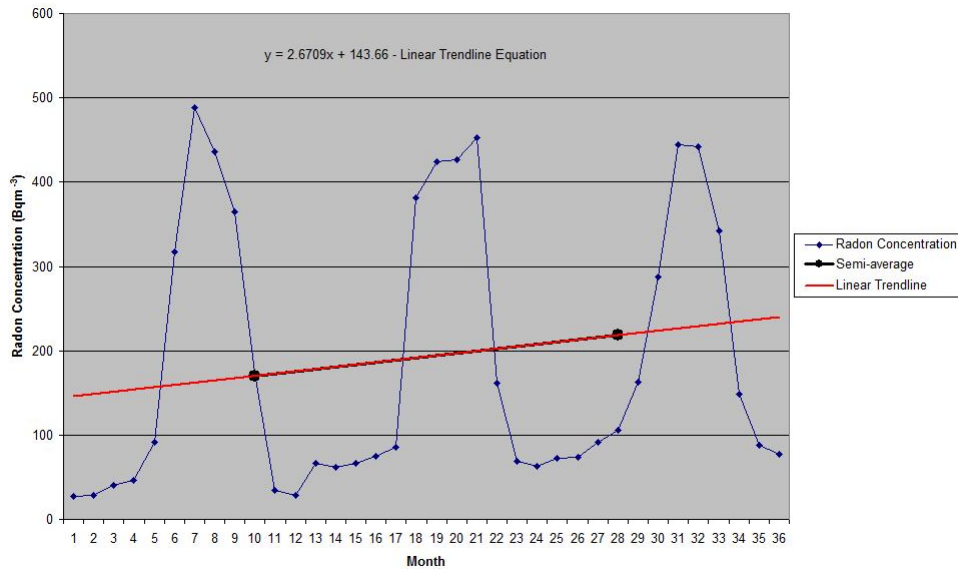


Figure 4.1: Nerja Caves (2011) - Semi-average

## 4.1 Moving Averages

Having chosen the Nerja (2011) dataset as the basis for the forecast model the first step is to analyse the data and identify the optimum trendline. As a starting point we calculate the semi-average, taking the average of the two halves of the data. The averages are then plotted on a graph with the original data and a linear trendline is inserted using the Microsoft Excel inbuilt process to obtain the equation of the semi-average line, as shown in Figure 4.1. Differentiating the equation gives the gradient of the line as 2.6709. This trendline is a reasonable approximation of the trend in the radon concentration but it appears to be a bit too steep for forecasting future concentrations as it is unlikely that concentrations would continue to rise at this rate over a number of years and is possibly influenced by the fact that the radon concentrations are from three different positions in the cave. In order to find a more representative trendline for the data we moved on to calculating the moving average for the data.

Microsoft Excel was used to plot moving averages for a range of periods from 2 to 12 months. The resulting plot is shown in Figure 4.2. The lower period moving averages simply mirror the curve of the data, once a period of 6 months is reached the moving average is beginning to smooth out the effect of the seasonal variation. The twelve period moving average averages a whole

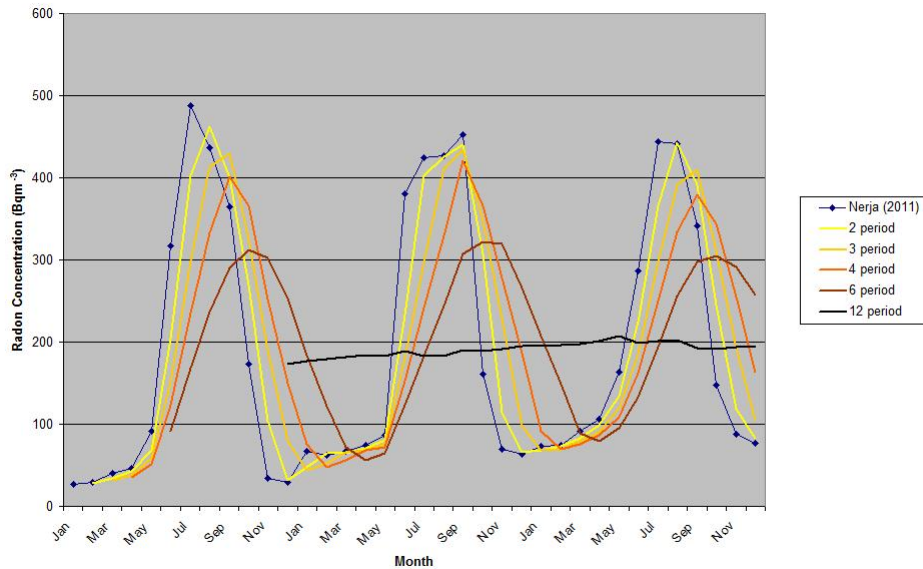


Figure 4.2: Nerja Caves (2011) - Moving Averages

year of results and the line becomes much flatter and is a good indication of the overall trend of the data with the seasonal variation removed. To confirm this conclusion the 13 period moving average was plotted and this began to reintroduce the seasonal variations, hence, the twelve period moving average was the best option.

The plot produced by Microsoft Excel, whilst sufficient for the identification of the trend, was not suitable for using to base the forecast model on. This was because it was not the centred moving average as the line started at the twelve month point, not the seventh month as would be the case for the centred moving average. Similarly its last value was at thirty-six months rather than thirty. The centred average was calculated from the base data (See Figure B.3) and plotted as shown in Figure 4.3. The use of the centred moving average allows for a comparison with the actual value of the data.

## 4.2 Curve Fitting

The next stage is to use the curve fitting capability of Microsoft Excel to identify the equations for a range of potential models. These are the linear, polynomial, power, exponential and log trendlines for the base data. Figure 4.4 shows the five trendlines plotted against the original data. The equations

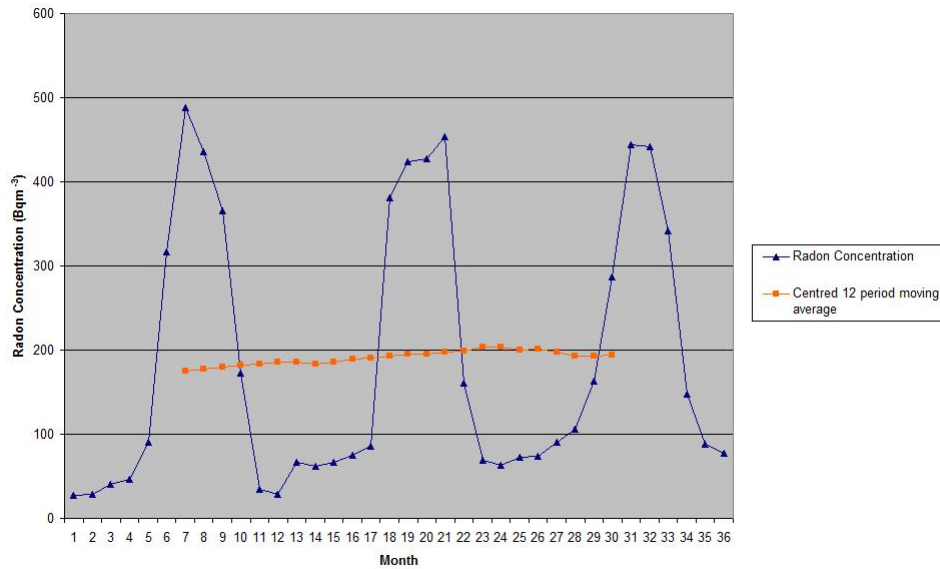


Figure 4.3: Nerja Caves (2011) - Centred Twelve Period Moving Average

Trendline	Equation
Linear	$y = 2.1126x + 148.28$
Polynomial	$y = -0.1998x^2 + 9.5066x + 101.45$
Power	$y = 41.857x^{0.4129}$
Exponential	$y = 77.974e^{0.0257x}$
Logarithmic	$y = 39.16 \ln(x) + 83.24$

Table 4.1: Trendline Equations

for the five trendlines are given in Table 4.1.

The time series for these five trendlines are calculated using the months 1 to 36 as the  $x$  values, see Figure B.4 for table of results. The errors for each of the trendline equations were then calculated by subtracting the trendline time series value for each month from the twelve period centred moving average, as the moving average has had the seasonal variations removed from it. The mean error, absolute mean error, mean squared error, absolute mean squared error and the standard deviation of the errors were then calculated for each of the trendlines. Table 4.2 summarises the results of these calculations (The full set of calculations can be found in Figures B.5 to B.8).

It is obvious from the table that the power and exponential trendlines

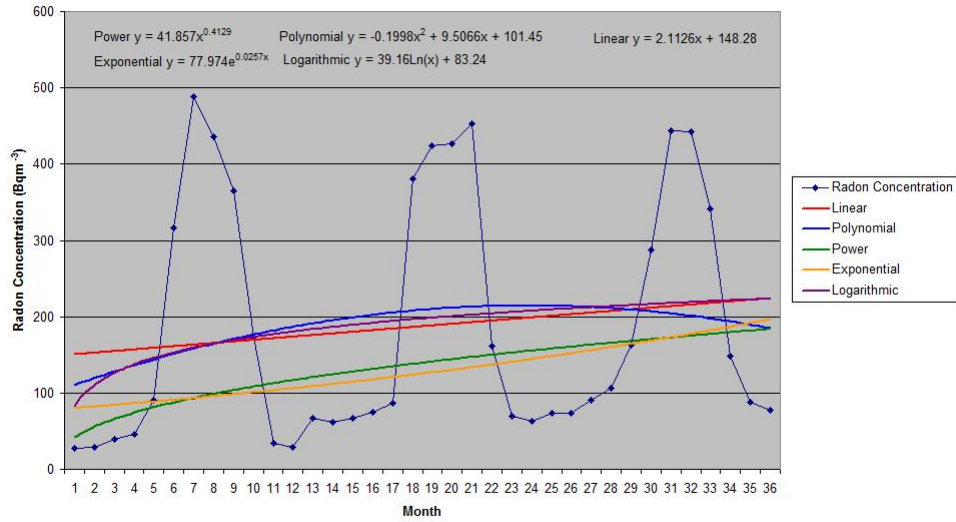


Figure 4.4: Nerja Caves (2011) - Trendlines

Error	Linear	Polynomial	Power	Exponential	Logarithmic
Mean	3.64	-8.37	53.98	63.57	-3.32
Absolute Mean	8.64	12.21	53.98	63.57	8.48
Mean Squared Square Root	9.75	13.01	56.36	65.77	10.60
Absolute Mean Squared Square Root	9.75	13.01	56.36	65.77	10.60

Table 4.2: Summary table of error calculations for trendlines

	Linear	Polynomial	Power	Exponential	Logarithmic
Standard Deviation	9.25	10.18	16.54	17.23	10.28

Table 4.3: Standard deviations for trendlines

have significantly greater errors than the other three, hence, these were discarded as options for the forecast model. This left the linear, polynomial and logarithmic trendlines. In the error table the Polynomial consistently gave higher results than both the linear and logarithmic trendlines although they values were relatively close. The polynomial was also dismissed as an option. The remaining two trendlines were much closer and neither were consistently lower than the other. The logarithmic trendline mean error was smaller than the mean error for the linear trendline, however, the linear trendline had lower values for all other calculated errors. It would appear from this that the linear trendline would be the favoured option for the forecast model but given that the linear and logarithmic were so close, some further analysis was carried out, starting with the standard deviation of the errors. Table 4.3 gives the standard deviation of the errors for the trendlines, for completeness all five trendlines have been included.

Once again the results for the power and exponential trendlines were significantly greater than the others. The polynomial trendline standard deviation was actually smaller than that for the logarithmic trendline, but, as with the majority of the error calculations, the linear trendline standard deviation was the smaller of the three. This added to the evidence that the linear trendline was the leading option for use as the base for the forecast model.

The data analysis showed that the linear trendline is the closest approximation to the twelve period centred moving average as demonstrated by the results of error calculations and standard deviation. This equation will therefore be used for the forecast model.

# Chapter 5

## Forecast Model

### 5.1 Construction of the Model

The model type being used in this study is a relatively simple one. The basic structure of the model will be one of two types, additive or multiplicative. In an additive model it is assumed that the model is the sum of the time series components, as shown in equation 5.2, whereas in a multiplicative model the data is the product of the components. Having identified the model type we will identify the components of the model by taking out the trend that was calculated in the previous chapter. Having “taken apart” the data we will reconstruct it using the identified trend and variations to create a forecast for the data. This forecast will then be compared with the original data using quantitative error calculations, as in Chapter 4, to assess its accuracy. In this study we have more than one set of data for the cave in question and this additional data will be used as a “test” for the forecast model, again using error calculations. This will help to identify both the accuracy of the model and how it may be improved.

The graph in Figure 3.3 of the three years of data for the Nerja Caves shows that the three peaks and troughs are of roughly equivalent size rather than increasing in size on each iteration, which indicates that the model is an additive model rather than a multiplicative model. The additive model has the form,

$$X = T + C + S + I + e \quad (5.1)$$

where X is the outcome, T is the trend, C represents any cyclical effect, S is the seasonal variation, I is represents any irregular variations and e is the error. In this model only the trend and seasonal variation are present, plus any errors so the equation becomes .

Month	Seasonal Variation
Winter	-120.0208333
Spring	-8.965277778
Summer	245.5277778
Autumn	-104.875

Table 5.1: Average Seasonal Variations

$$X = T + S + e \quad (5.2)$$

The first step in constructing the forecast model is to identify the seasonal variation. This is done by subtracting the twelve period centred moving average from the original data between months 7 and 30 to obtain the monthly variation in radon concentrations (Figure B.9 shows this calculation). The monthly variations are then averaged over a three month period each representing a season, this gives us two values for each season which we then average to obtain a single value for each season as shown in Table 5.1.

The model is then constructed using the linear trendline values plus the seasonal variations given in Table 5.1, which gives a forecast radon measurement for each month as shown below (Calculation Table shown in Figure B.10).

$$\begin{aligned} \text{Radon Concentration} &= \text{Linear Trendline Equation} + \text{Seasonal Variation} \\ C_{Rn} &= (2.1126x + 148.28) + S_V \end{aligned} \quad (5.3)$$

Where  $C_{Rn}$  is the radon concentration in  $Bqm^{-3}$ ,  $x$  is the month and  $S_V$  is the seasonal variation for that month.

The forecast results are plotted alongside the original data in Figure 5.1. The graph shows that the forecast model is a reasonably good fit to the original data. The use of seasonal variation values results in plateaux at each season, at some points these fit well with the original data, such as during the winter period, but at others, noticeably during spring, the plateau does not reflect the real situation of a sharp rise in radon concentration values. The errors between the forecast and the original data were calculated, the result was a mean error of 2.92 and a mean squared error of 68.12 (See Figure B.12). The large mean squared error is due to the relatively large differences caused by the plateaux.

To try and reduce the error margins and produce a smoother curve for the forecast model we calculated the monthly averages from the monthly

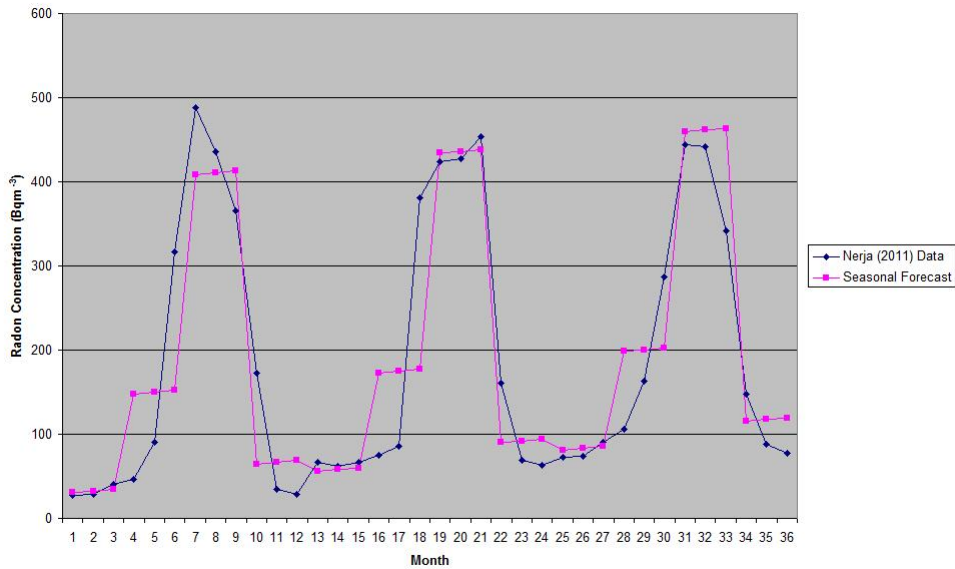


Figure 5.1: Nerja Caves (2011) - Seasonal Forecast Model Results Comparison

variation figures and applied them to the model in place of the seasonal averages, still using the same linear trendline equation, see Figure B.11. As previously, the forecast results are plotted against the original data to see how good a fit they are, Figure 5.2. Visually the resulting curve is much smoother and a much better fit to the original data. The plateaux have disappeared and the forecast follows the original data closely with the exception of the summer period where variations from year to year are more disparate. The mean and mean squared errors were calculated as for the seasonal model. The mean error was the same as would be expected as both models are based on the same data, however, the mean squared error is much smaller at 29.48 compared with 68.18, indicating that the monthly model is a better fit to the original data than the seasonal variation model. Hence the monthly variation model will be used as the main model.

The results of the comparison of the model confirm that the additive model was the right choice for this model and that the linear trendline is a good choice to base the model on. Having constructed the model and tested it against the original data we will now proceed by comparing the model results against other data from the same cave system.

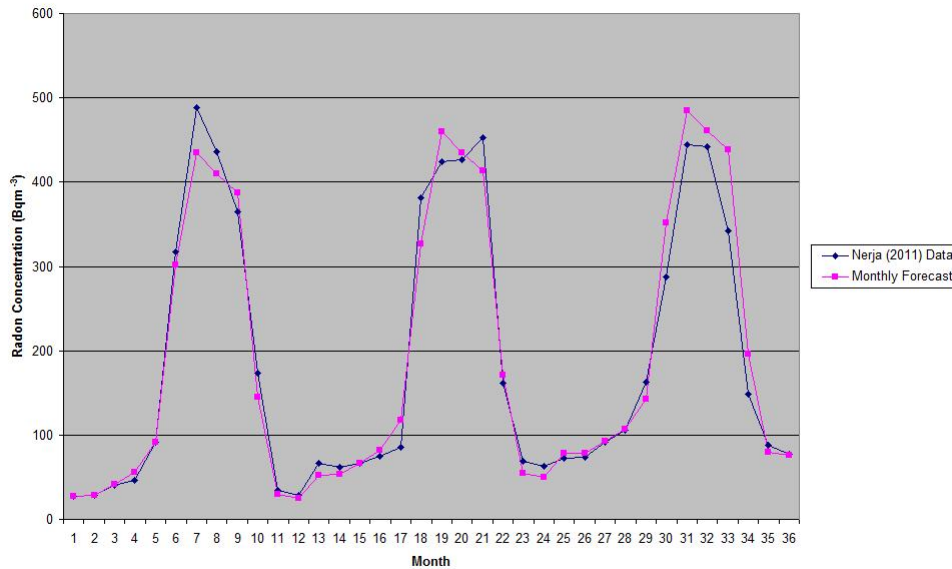


Figure 5.2: Nerja Caves (2011) - Monthly Forecast Model Results Comparison

## 5.2 Comparison with other Nerja Data

The Dueñas et al. (2011) paper [6] is not the only paper to contain radon concentration data for the Nerja Caves and this data can be used to test the robustness of the model. Two other papers Dueñas et al. (1999) [4] and Dueñas et al. (2005) [5] have monitoring data from the Nerja Cave system, [4] contains Spring-Summer and Autumn-Winter arithmetic means for four individual halls and [5] has one years worth of data for the Ballet Hall in monthly averages. Both of these sets of data can be used in different ways to examine the forecast model.

The monthly forecast model results can be used to find values for the Spring-Summer and Autumn-Winter averages that can then be compared with the results given in [4]. Table 5.2 shows both sets of results for comparison.

At first glance these results are not encouraging as the majority of the forecast values are far higher than the actuals, however, these values must be treated with caution. The paper does not give any details of the base data or the dates considered to constitute Spring-Summer and Autumn-Winter. Our calculations took Spring-Summer to be April to September inclusive, giving an average value of 306 as above, but if Spring-Summer is taken to be March

	Spring-Summer	Autumn-Winter
Model Total	306	75
Model Year 1	280	50
Model Year 2	305	71
Model Year 3	330	100
Vestibule	151	22
Ballet	176	52
Mirador	168	56
C. Hercules	177	62

Table 5.2: Half year average radon concentrations

to August inclusive the value drops to 248 which is lower than any of the average model values above. It is possible that the conditions were different during the measurements in the 1999 paper. this may well be the case as if the average for Spring-Summer is calculated for the original data in [6] it comes out at 299, considerably higher than any of the values from [4]. If we calculate the average of the Spring-Summer and Autumn-Winter values and calculate the ratios for the [4] paper and do the same for the forecast model the resulting ratios are 3.5/1 and 4/1 which are reasonably close and show that the seasonal variations in the two sets of data are similar.

The next step is to compare the forecast results with the Nerja 2005 dataset. The Nerja 2005 dataset is very close, though not identical, to the second year of data in the Nerja 2011 dataset. Dueñas et al (2005) [5] gives results for the Ballet Hall from July 2003 to June 2004 and Dueñas et al (2011) [6] gives values for the Ballet Hall from January 2004 to December 2005, hence there is some overlap in the data, however, this will show the effect of comparing the first years results of the forecast model with the second year of original data, or very close to it. Figure 5.3 shows the results of this comparison.

The curve of the forecast model is a reasonably good fit to the Nerja 2005 data but the Winter and Spring values are generally underestimated. The Summer values are less consistent with some overestimated by approximately 50 and others underestimated by a similar amount. The underestimate of the Winter and Spring values may be due to the fact that the gradient of the linear trendline is 2.1126, this is a good basis for the three year comparison with the Nerja 2011 dataset. Over a single year the linear trendline will have a positive gradient as the concentrations are low for the first five months followed by five months of high concentrations causing the distribution to

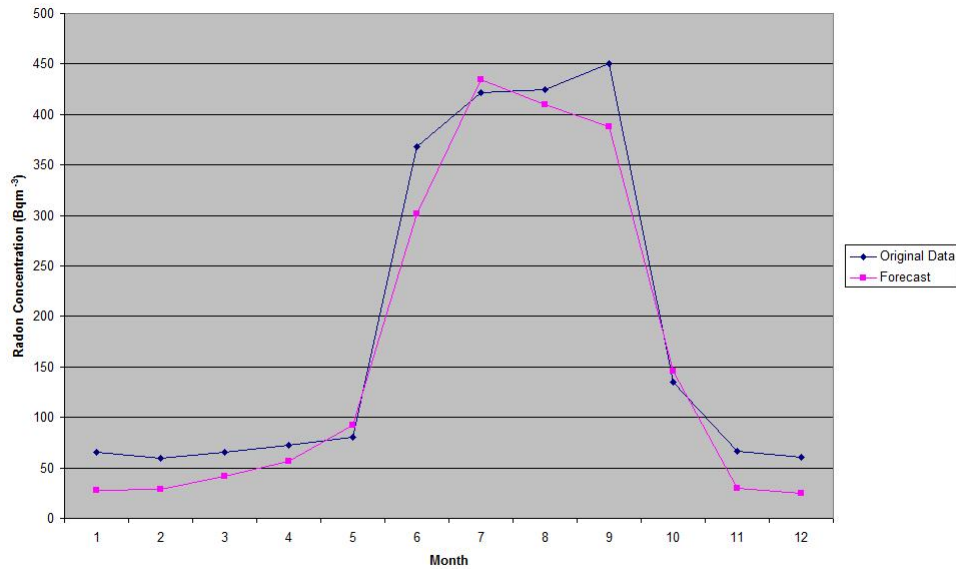


Figure 5.3: Nerja Caves (2005) - Monthly Forecast Model Results

be skewed. However, as a model to be used as a general tool for forecasting radon concentrations in caves a trendline with a zero gradient may be more appropriate as a basis for the model. This may give a better representation of the year to year conditions rather than this trendline which, as noted in Chapter 3, is based on three different monitoring positions within a cave system which may have created an artificial gradient that would not necessarily appear in reality.

The mean error and the mean squared error were calculated for the forecast model against the Nerja 2005 dataset (The calculation table can be found in Figure B.13). The mean error is 24.15 which is much larger than the -2.92 achieved for the Nerja 2011 dataset however, the mean squared error is 35.10 which is much closer to the 29.48 obtained for the Nerja 2011 dataset.

### 5.3 Summary

Comparing the forecast model with other data from the same cave system has given some useful insights to the variations from year to year in the Nerja caves. The monthly variation model gives a much better fit to the Nerja 2001 dataset than the seasonal variation model, which produced plateaux.

Comparison with the Nerja 1999 and 2005 data highlights the differences between different years, especially in the case of the 1999 data. Whilst the ratios of Spring-Summer to Autumn-Winter averages are reasonably close for the forecast model and the 1999 data the actual half yearly averages are considerably different as is the overall average. The comparison with the Nerja 2005 dataset demonstrates the need to have an appropriate trendline for the model, which is not biased by either differences in conditions from year to year or by the effect of different monitoring positions within the cave system. One way forward may be to use a trendline with a zero gradient, perhaps using the annual average concentration for the cave, and find the seasonal or monthly variations from that basis.

## Chapter 6

# Comparison Against other Datasets

The Nerja 2011 forecast model will now be compared with four other datasets identified in the literature review, these are Niedźwiedzia, Radochowska, Altamira and Domic. Some adjustments will be necessary to allow the model results and the comparison dataset to be compared on the same graph. Any adjustments made will be fully described and the reason for them explained.

The first comparison dataset is from [25] and is for the Niedźwiedzia cave system. The measurements start in July and hence the model results from month seven onwards were used for a period of two years. Measurements were taken in seven of Niedźwiedzia's halls, and an overall average calculated. To gain an overall picture of the comparison the average data for Niedźwiedzia is used rather than for a particular hall. The data for Niedźwiedzia is measured in  $kBqm^{-3}$  whereas the forecast data using the Nerja 2011 model is in  $Bqm^{-3}$ , in Figure 6.1 both sets of data are presented in  $Bqm^{-3}$ . The first eighteen months of the forecast broadly reflect the curve of the data for the cave system. Beyond that point the third peak appears much earlier in the year than in the forecast. It is difficult to tell how different the two curves actually are because of the difference in the magnitude of the two sets of data.

In order to show the two sets of data in a way that allows a qualitative analysis, Figure 6.2, the Niedźwiedzia data has been left in  $kBqm^{-3}$  then multiplied by 100. This means that the y-axis label only applies to the forecast model data. This adjustment allows a closer comparison of the general shape of the two curves.

Figure 6.2 shows much more clearly the difference in the two curves, although the curves are still similar for the first eighteen months this graph shows that the peak values of radon concentration in the Niedźwiedzia cave

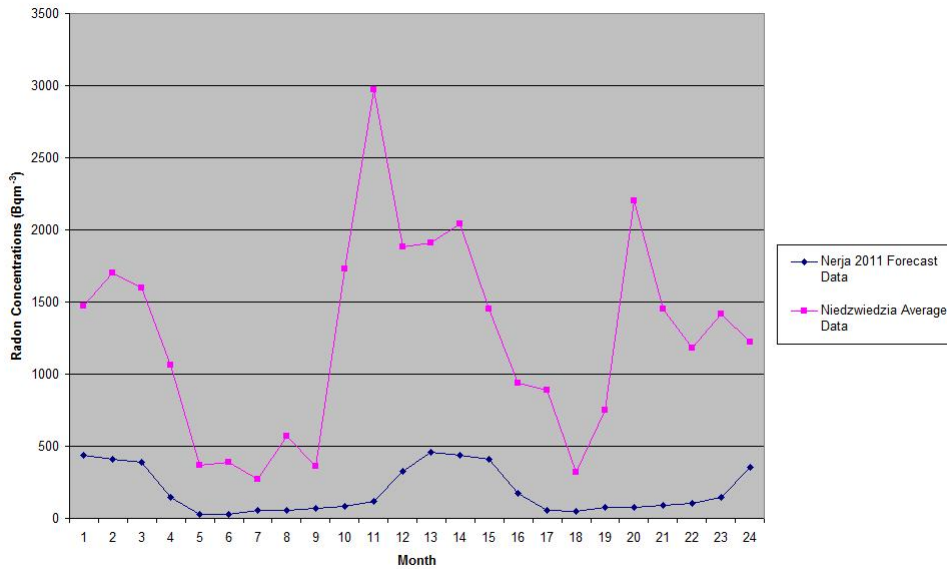


Figure 6.1: Nerja Caves 2011 Forecast v. Niedźwiedzia Average Data

occur two to four months earlier than in the Nerja 2011 forecast and the difference between the winter and summer levels is much greater. The timing of the minimum values however do appear to coincide quite well. It is possible that this difference in the seasonal timing is related to the different geographical locations of the two caves, Nerja in Spain and Niedźwiedzia in Poland, as these may have subtly different seasonal variations. The difference in winter to summer values may also be related to the cave location and local weather (temperature) patterns. Overall, in the qualitative analysis, the Nerja 2011 forecast model and the Niedźwiedzia data have the same “shape” and mirrors the seasonal variations of the Niedźwiedzia cave reasonably well, although differences of scale in the measurements and the earlier peaks in the Niedźwiedzia cave certainly raise some interesting questions relating to cave location and seasonal timings and the potential for a further study.

The second dataset to be compared with the model is from the same paper, [25], as the Niedźwiedzia cave data. It is from the Radochowska Cave system, also in Poland. As with the Niedźwiedzia cave the measurements for the Radochowska cave are measured in  $kBqm^{-3}$ , but they are not as high as for Niedźwiedzia so the data has simply been converted to  $Bqm^{-3}$  before being plotted on to the same graph, Figure 6.3. The data for Radochowska cave starts in September so the values from the 9th month onwards have been used from the model.

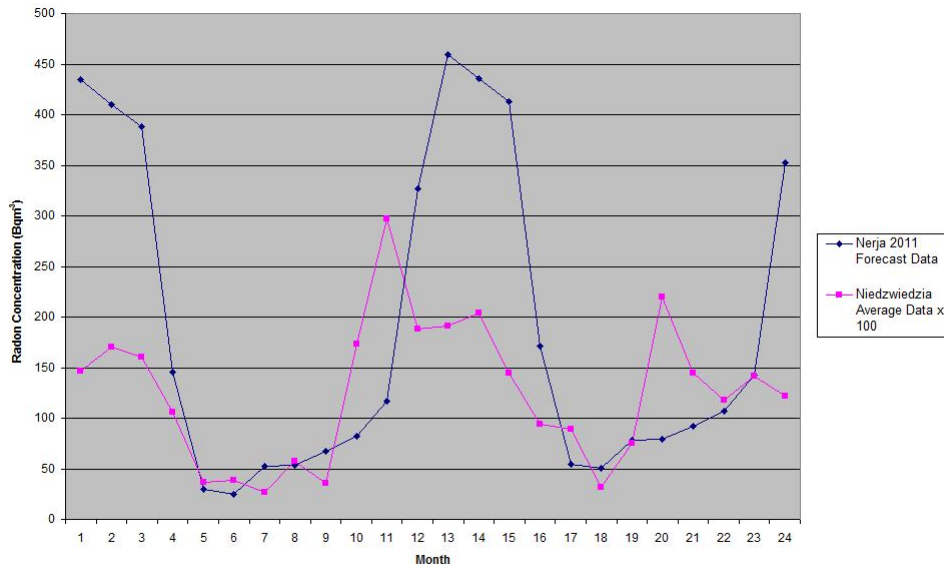


Figure 6.2: Nerja Caves 2011 Forecast v. Niedzwiedzia Average Data (Adjusted)

The forecast model curve once again is in broad agreement with the measured data. For the October to April period the levels are similar and it is only during the Spring/Summer period that the values diverge, the Radochowska data rising sharply earlier than the model and, as with Niedzwiedzia cave getting much higher than the Nerja 2011 model predicts. This potentially adds weight to the theory that the timing of the seasonal variations and the local weather conditions mean that the model cannot be transferred without being adjusted to account for the ratio of Winter to Summer radon concentrations, perhaps using the link with outside temperature identified in the Literature Review.

The next dataset for comparison may produce more evidence for the theory that the location of the cave has a significant effect on the Winter/Summer ratios of radon concentrations. The Altamira Cave is located in Spain, as is the Nerja Cave that the model is based on, however it displays the opposite pattern of seasonal variations to the majority of caves, in Summer the radon concentrations are at their lowest and in the Winter they are at their peak. In order to compare this data with the Nerja 2011 forecast model the model results are adjusted by six months to fit with the peaks and troughs of the Altamira dataset. As the Altamira results are an order of magnitude greater than the forecast results the model results have

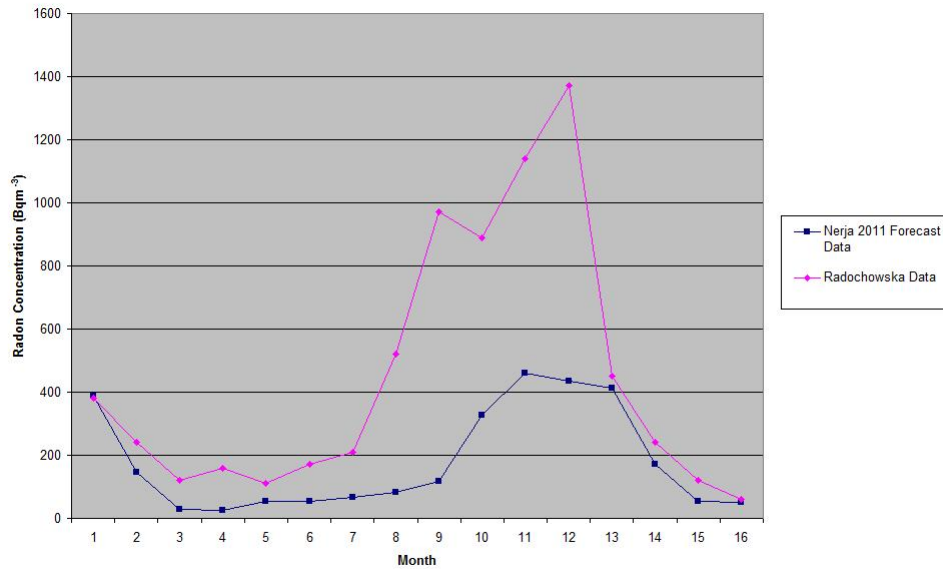


Figure 6.3: Nerja Caves 2011 Forecast v. Radochowska Data

been multiplied by 10 to allow a qualitative analysis. The resulting graph is shown in Figure 6.4.

The two caves have roughly the same shape when the forecast model is multiplied by a factor of ten but with the forecast data having a flatter low radon concentration period. What this comparison does show is that the agreement is much closer when the caves are located in the same country, although this could not be confirmed without obtaining data from other Spanish caves. It also shows that the model can be used for the opposite seasonal pattern than the one it was based on with the appropriate adjustments.

The final dataset for comparison is the Domica data set. The Domica Cave is in Slovakia and appears, from the small amount of data available, to follow the high Summer/low Winter radon concentration pattern of the majority of caves. The Domica data starts in July so, as previously, the model forecast from the seventh month on is used for comparison. On this occasion the forecast model data is multiplied by a factor of two to allow a comparison graph to be produced, see Figure 6.5.

It is difficult to draw many conclusions from the graph as we only have six months of data to compare. The latter half of the graph has a similar shape but the a peak in September (Month 3) is not mirrored in the forecast data. Without more information it would be unwise to try and draw any

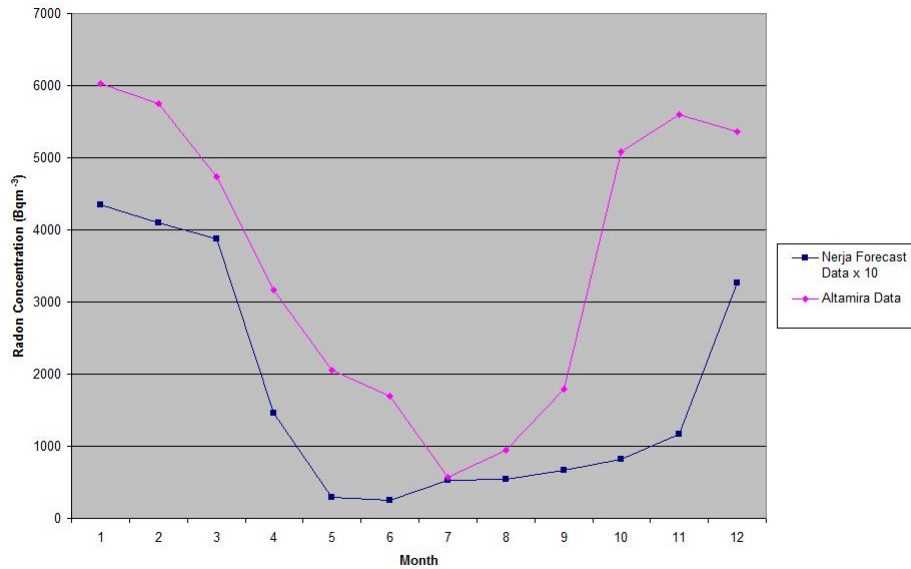


Figure 6.4: Nerja Caves 2011 Forecast v. Altamira Data

conclusions from the comparison other than to note the downward trend towards the latter part of the graph.

The figures in this chapter demonstrate that the method used to construct the forecast model is robust enough to produce a general agreement with the seasonal variations in other caves although the actual results need some adjustment to make them comparable. The comparison with other datasets is also a useful tool in highlighting a number of issues that would need to be addressed if the forecast model were to be developed for use with other caves. The key points are;

- A reference point from the cave would be needed to identify the level of radon concentrations, for instance whether they are measured in  $kBqm^{-3}$  or  $Bqm^{-3}$ , or the annual average radon concentration,
- The ratio of Winter/Summer ratios of either radon concentrations or outside temperature would need to be fed in to the model to improve the peak forecasts,
- Further work examining the possible variation in seasonal timings for different countries would be needed to improve the accuracy of the seasonal variations in the model.

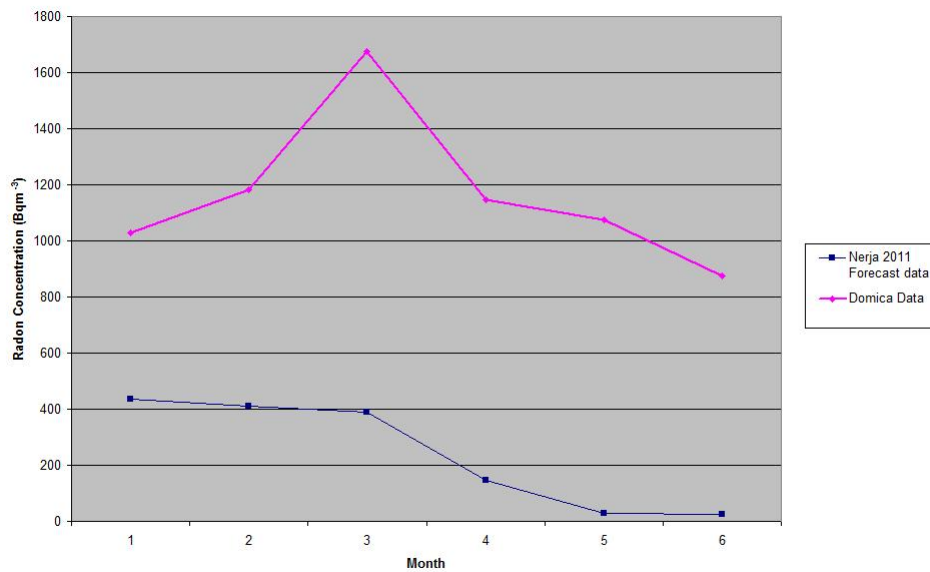


Figure 6.5: Nerja Caves 2011 Forecast v. Domica Data

- Investigation of other factors that could affect the radon concentrations would be necessary such as the presence of running water or flooding events.

Mean error calculations, etc., have not been carried out on the comparisons in this chapter as the difference in magnitude between the forecast model results and the original data would make the calculations meaningless.

# Chapter 7

## Discussion

The results of the forecast model as a prototype method on the Nerja 2011 dataset are broadly encouraging regarding the use of this method and indeed this model for other caves. The Nerja 2011 dataset has the longest overall period of measurement and this resulted in a seasonal variation pattern that fits the data well when the monthly values are used. It should be noted that the gradient of the linear trendline, although it is the best fit to the twelve period moving average data, is possibly influenced by both the particular weather conditions of the three years of measurement and the position of the measurements within the cave. If the method were to be used in a more generic way on other caves it may be advisable to obtain data which results in a flat trendline, i.e. assumes that the seasonal variation is the only factor affecting the data, and calculate the seasonal or monthly variations with respect to that, hence eliminating any influences specific to the Nerja Caves system.

An assumption was made based on observation of the three years of data, Figure 3.3, that the model is an additive model as described in equation 5.2. The results of the model demonstrate that this is indeed the case with only the trend, seasonal variation and error being present for the Nerja Cave system. Although the main conclusion of an additive model holds true for the comparison datasets, differences in the magnitude of the results and differences in the timing of the seasons meant that the results were not as close. However the general shape of the model was sufficiently close to the shape of the comparison data to show that there is merit in the use of this method and the possibility of it being developed to be used as a generic tool for forecasting radon concentrations in other caves

The method that has been applied here of calculating a trendline and the seasonal variations to forecast the radon concentration as a time series has produced sufficiently good results against the original cave that the use of

this method on other caves would be a good starting point for identifying the particular features of their seasonal, and possibly other, variations in radon concentrations. If, for instance a cave suffered from flooding or the radon concentrations are affected by radon bursts due to seismic activity, it may be possible to introduce these to the model as an irregular variation.

Taking the comparisons with other datasets into account, if the model were to be developed further to make it into a generic model a reference point for the range of values would need to be inserted to the model. Examining the results of the comparison graphs, Figures 6.1 to 6.5, some options would be an annual average or ratios of Winter/Summer radon concentrations or outside temperature values. An alternative approach may be to use percentages rather than fixed values. The other main difference highlighted in the comparison graphs is the difference in the start dates for seasons in different countries, this may be a false result as data from only three countries in Europe has been considered but the differences were marked enough that it would be worth further investigation if the model were to be developed.

Overall the method and resulting model produced good results for the cave system that it was based on, and broadly similar seasonal patterns for other caves. However, a considerable amount of further work would be needed if it was to be used to predict concentrations in other caves.

# Chapter 8

## Conclusions

This study details the development of a forecast model to predict the radon concentration build up in a visitor caves over a period of time to identify the seasonal variations. It includes a literature review to identify any existing modelling of radon concentrations in visitor caves and to search for a dataset suitable for use as a base for the model and the creation of a forecast model and statistical analysis of its results.

The method used to develop the forecast model is shown to be suitable, with good agreement when tested against the original data and reasonable agreement with other measurements for the same cave. The comparison of the forecast model with other datasets is less convincing, although there is broad agreement on the seasonal variations, differences in the magnitude of radon concentrations and the ratio of Winter to Summer concentrations highlight the need for further investigations. This model is a relatively simple one and the results of this analysis supports the conclusion that in order for the model to be used to predict radon concentrations in other caves further development would be needed, as discussed in the Further Work chapter of this report.

Overall the method is shown to be a sound basis for forecasting radon concentration seasonal variations and if developed further it could possibly be used to predict maximum concentrations in a visitor cave and hence, reduce the number of measurements needed in caves.

# Chapter 9

## Further Work

A number of areas of further study were identified in the course of this study, mainly concerned with developing the model to allow it to be used to forecast radon concentrations in other caves. These potential developments are outlined below.

- The use of a linear trendline is reasonably successful for the cave that the model is based on, but in order to develop the model further the use of a stationary time series as the basis for the model may be a better option. This is because it would eliminate any bias introduced due to position of the monitoring equipment used to collect the base data or due to the temperature pattern over the time period of the monitoring. A flat trendline, using for instance the annual average value of all the monitoring results for a cave, would allow the seasonal or monthly variations to be calculated in relation to a trendline that would have the same gradient no matter which cave it was applied to.
- It would be a useful exercise to use the same method on other cave systems for which data is available to create cave specific models and test them against their base data to see whether the results are as promising as for the Nerja cave system. This may also help in identifying the features that would be important in developing a generic model for radon in visitor caves.
- The concept of a stationary time series would also allow a reference point for the forecast to be established. As noted in the discussion the radon concentrations can vary by orders of magnitude from cave to cave. This causes a problem for the forecast model, leading to adjustments having to be made post forecast. A method whereby a reference point for the model can be inserted to allow the forecast to be

scaled appropriately would remove this necessity and improve the forecast. Possible options for this could be the annual average of radon concentrations, the use of percentages rather than fixed values or the Winter/Summer concentration or temperature ratios.

- The comparison with other datasets highlighted an apparent difference in the seasonal timings in different countries, although this observation is based on data from only three countries. Investigating the timing of seasons across Europe or even worldwide may allow for the model to be refined to reflect the potential difference in seasonal variations in different regions. Examining the radon concentrations in caves in the southern hemisphere would identify whether the model could be used simply by shifting the forecast by six months (As was done in the case of the Altamira data due to a high Winter, low Summer concentration pattern).
- Having established that the model for radon concentrations in visitor caves is an additive model, that addition of an irregular trend to take account of events such as flooding or heavy rains that have an effect on radon concentrations in some caves. Given the link demonstrated between radon “bursts” in some caves and seismic activity this could also be considered as an irregular trend.

# Appendix A

## Datasets

Month	Radon Concentration ( $Bqm^{-3}$ )		
	Average	Maximum	Minimum
January	65	113	32
February	60	132	31
March	65	125	29
April	72	179	34
May	80	283	39
June	368	575	155
July	422	544	342
August	425	525	210
September	450	568	235
October	135	538	51
November	66	159	35
December	61	118	28

Table A.1: Nerja 2005 Dataset

Month	Radon Concentration ( $Bqm^{-3}$ )		
	Vestibule	Ballet	Mirador
January	27	67	73
February	29	62	74
March	40	67	91
April	46	75	106
May	91	86	163
June	317	381	287
July	488	424	444
August	436	427	442
September	365	453	342
October	173	161	148
November	34	69	88
December	29	63	77

Table A.2: Nerja 2011 Dataset

Month	Radon Concentration ( $kBqm^{-3}$ )					
	Hall 1			Hall 2		
	a	b	c	a	b	c
July	1.26	1.56	1.25	1.56	1.56	1.50
August	2.15		1.55	1.88	1.49	2.08
September	1.75	1.53		1.80	1.75	1.59
October	1.36	0.74	0.88	1.17	1.53	1.00
November	1.16	0.28	0.28	0.26	0.46	0.36
December	1.17	0.60	0.42	0.30	0.40	0.36
January	0.71	0.80	0.34	0.17	0.16	0.24
February	1.39	0.92	0.74	0.48	0.44	0.52
March	1.16	0.83	0.42	0.28	0.25	0.30
April	2.50	2.30	1.23	2.27	1.91	1.89
May	3.57	2.27	2.29	2.92	2.94	3.03
June	2.24		2.29	2.65	2.07	1.82
July			1.50	2.01		
August			1.74	2.03		
September			1.54	1.72		
October			0.75	0.66		
November			1.02	1.05		
December			0.39	0.35		
January			1.01	0.83		
February			1.82	2.13		
March			1.00	4.18		
April			1.52	1.23		
May			1.28	1.76		
June			1.24	1.11		

Table A.3: Niedźwiedzia Dataset - Halls 1 and 2

Month	Radon Concentration ( $kBqm^{-3}$ )					
	Hall 3			Hall 4		
	a	b	c	a	b	c
July	1.26	2.02	1.34	1.59	1.34	2.04
August	1.86	1.59	1.74	1.89	1.51	1.64
September	1.58	1.60	1.80	1.65	1.55	1.61
October	1.12	1.33	1.31	0.90	0.83	1.18
November	0.35	0.46	0.36	0.35	0.25	0.26
December	0.31	0.36	0.29	0.33	0.25	0.26
January	0.15	0.17	0.18	0.16	0.16	0.14
February	0.48	0.55	0.46	0.40	0.31	0.33
March	0.22	0.24	0.21	0.22	0.19	0.22
April	1.41	1.91	1.88	2.04	1.08	1.66
May	2.92	3.53	3.45	2.67		3.60
June	2.05	1.69	1.51	2.38	1.35	1.75
July		2.43			1.96	
August		2.42			1.77	
September		1.40			1.11	
October		1.25			0.96	
November		0.83			0.84	
December		0.19			0.29	
January		0.59			0.50	
February		2.61			1.48	
March		0.97			0.8	
April		1.10			1.58	
May		1.49			1.21	
June		1.10			1.06	

Table A.4: Niedźwiedzia Dataset - Halls 3 and 4

Month	Radon Concentration ( $kBqm^{-3}$ )					
	Hall 5			Hall 6	Hall 7	Average
	a	b	c			
July	1.06	1.03	1.72			1.47
August	1.43	1.43	1.54			1.70
September	1.15		1.41			1.60
October	0.61	0.91	1.02			1.06
November	0.18	0.21	0.36			0.37
December	0.26	0.18	0.42			0.39
January	0.27	0.10	0.37	0.23		0.27
February	0.29	0.61	0.60	0.67		0.57
March	0.22	0.26	0.25	0.45		0.36
April	1.06	1.26	1.02	2.21		1.73
May		2.26		3.15		2.97
June	1.19	1.18	1.61	2.43		1.88
July	1.70			1.90	1.88	1.91
August	1.38			2.82	2.14	2.04
September	0.88			1.49	2.04	1.45
October	0.68			1.08	1.20	0.94
November	0.59			1.13	0.74	0.89
December	0.23			0.45	0.35	0.32
January	0.59			0.88	0.84	0.75
February	2.14			2.63	2.61	2.20
March	0.81			0.79	1.61	1.45
April	0.51			1.15	1.14	1.18
May	1.08			1.62	1.53	1.42
June	0.73			1.90	1.38	1.22

Table A.5: Niedźwiedzia Dataset - Halls 5, 6, 7 and Average

Month	Radon Concentration ( $kBqm^{-3}$ )
September	0.38
October	0.24
November	0.12
December	0.16
January	0.11
February	0.17
March	0.21
April	0.52
May	0.97
June	0.89
July	1.14
August	1.37
September	0.45
October	0.24
November	0.12
December	0.06

Table A.6: Radochowska Dataset

Month	Radon Concentration ( $Bqm^{-3}$ )
February	6026
March	5756
April	4738
May	3162
June	2053
July	1694
August	574
September	940
October	1798
November	5079
December	5596
January	5357

Table A.7: Altamira Dataset

Month	Radon Concentration ( $Bqm^{-3}$ )	
	Average	Median
July	1027.06	1008.17
August	1180.88	1190.25
September	1674.86	1644.50
October	1146.40	1141.38
November	1075.98	954.98
December	875.00	893.17

Table A.8: Domica Dataset

# Appendix B

## Calculations

Month	Hall 1	Hall 2	Hall 3	Hall 4	Hall 5	Hall 6	Hall 7
Jul	1.3925	1.6575	1.7625	1.7325	1.3775	1.9	1.88
Aug	1.813333	1.87	1.9025	1.7025	1.445	2.82	2.14
Sep	1.606667	1.715	1.595	1.48	1.146667	1.49	2.04
Oct	0.9325	1.09	1.2525	0.9675	0.805	1.08	1.2
Nov	0.685	0.5325	0.5	0.425	0.335	1.13	0.74
Dec	0.645	0.3525	0.2875	0.2825	0.2725	0.45	0.35
Jan	0.715	0.35	0.2725	0.24	0.3325	0.555	0.84
Feb	1.2175	0.8925	1.025	0.63	0.91	1.65	2.61
Mar	0.8525	1.2525	0.41	0.3575	0.385	0.62	1.61
Apr	1.8875	1.825	1.575	1.59	0.9625	1.68	1.14
May	2.3525	2.6625	2.8475	2.493333	1.67	2.385	1.53
Jun	1.923333	1.9125	1.5875	1.635	1.1775	2.165	1.38

Figure B.1: Niedźwiedzia Cave - Averaged Monthly Data

Anova: Two-Factor Without Replication						
SUMMARY	Count	Sum	Average	Variance		
Row 1	7	11.7025	1.671785714	0.045359821		
Row 2	7	13.69333333	1.956190476	0.189391171		
Row 3	7	11.07333333	1.581904762	0.072768915		
Row 4	7	7.3275	1.046785714	0.024428571		
Row 5	7	4.3475	0.621071429	0.070003869		
Row 6	7	2.64	0.377142857	0.01772381		
Row 7	7	3.305	0.472142857	0.054888393		
Row 8	7	8.935	1.276428571	0.447366369		
Row 9	7	5.4875	0.783928571	0.235722619		
Row 10	7	10.66	1.522857143	0.119459226		
Row 11	7	15.94083333	2.277261905	0.244117063		
Row 12	7	11.78083333	1.68297619	0.116919643		
Column 1	12	16.02333333	1.335277778	0.33492984		
Column 2	12	16.1125	1.342708333	0.519268703		
Column 3	12	15.0175	1.251458333	0.616326657		
Column 4	12	13.53583333	1.127986111	0.547187305		
Column 5	12	10.81916667	0.901597222	0.233549553		
Column 6	12	17.925	1.49375	0.569600568		
Column 7	12	17.46	1.455	0.421463636		
ANOVA						
Source of Variation	SS	df	MS	F	P-value	F crit
Rows	28.83697943	11	2.621543585	25.33779061	1.50233E-19	1.936958128
Columns	3.000287368	6	0.500047895	4.833071982	0.000381971	2.239479537
Error	6.828609458	66	0.10346378			
Total	38.66587626	83				

Figure B.2: Niedźwiedzia Cave - ANOVA Two Factor Without Replication Results

Month	Radon Concentration	12 Period Moving Averages	Centred 12 Period Moving Average
1	27		
2	29		
3	40		
4	46		
5	91		
6	317	172.9166667	
7	488	176.25	174.5833333
8	436	179	177.625
9	365	181.25	180.125
10	173	183.6666667	182.4583333
11	34	183.25	183.4583333
12	29	188.5833333	185.9166667
13	67	183.25	185.9166667
14	62	182.5	182.875
15	67	189.8333333	186.1666667
16	75	188.8333333	189.3333333
17	86	191.75	190.2916667
18	381	194.5833333	193.1666667
19	424	195.0833333	194.8333333
20	427	196.0833333	195.5833333
21	453	198.0833333	197.0833333
22	161	200.6666667	199.375
23	69	207.0833333	203.875
24	63	199.25	203.1666667
25	73	200.9166667	200.0833333
26	74	202.1666667	201.5416667
27	91	192.9166667	197.5416667
28	106	191.8333333	192.375
29	163	193.4166667	192.625
30	287	194.5833333	194
31	444		
32	442		
33	342		
34	148		
35	88		
36	77		

Figure B.3: Nerja Caves - 12 Period Centred Moving Average

Linear	Polynomial	Power	Exponential	Logarithmic
150.3926	110.7568	41.857	80.00390434	83.24
152.5052	119.664	55.72670736	82.08665338	110.3836436
154.6178	128.1716	65.88271139	84.22362281	126.2616572
156.7304	136.2796	74.19227162	86.41622416	137.5272872
158.843	143.988	81.35285766	88.6659057	146.2655887
160.9556	151.2968	87.71356231	90.97415342	153.4053008
163.0682	158.206	93.47792831	93.34249196	159.4418414
165.1808	164.7156	98.77657283	95.77248567	164.6709308
167.2934	170.8256	103.6990625	98.26573964	169.2833144
169.406	176.536	108.3098858	100.8239007	173.4092322
171.5186	181.8468	112.6572479	103.4486586	177.1415789
173.6312	186.758	116.7782693	106.1417471	180.5489444
175.7438	191.2696	120.702234	108.904945	183.6834168
177.8564	195.3816	124.4527117	111.7400775	186.585485
179.969	199.094	128.0489964	114.6490173	189.2872459
182.0816	202.4068	131.5071116	117.6336857	191.8145744
184.1942	205.32	134.8405321	120.6960543	194.1886346
186.3068	207.8336	138.0607141	123.8381459	196.426958
188.4194	209.9476	141.1774912	127.0620358	198.5442304
190.532	211.662	144.1993768	130.3698535	200.5528758
192.6446	212.9768	147.1337977	133.7637839	202.4634987
194.7572	213.892	149.9872778	137.2460689	204.2852225
196.8698	214.4076	152.7655829	140.8190084	206.0259535
198.9824	214.5236	155.4738381	144.4849627	207.692588
201.095	214.24	158.1166221	148.2463531	209.2911773
203.2076	213.5568	160.6980451	152.1056641	210.8270604
205.3202	212.474	163.2218126	156.0654449	212.3049717
207.4328	210.9916	165.6912786	160.128311	213.7291286
209.5454	209.1096	168.1094903	164.2969461	215.1033047
211.658	206.828	170.4792257	168.5741037	216.4308895
213.7706	204.1468	172.8030253	172.9626089	217.7149389
215.8832	201.066	175.0832196	177.4653605	218.958218
217.9958	197.5856	177.3219522	182.0853326	220.1632361
220.1084	193.7056	179.5212001	186.8255769	221.3322781
222.221	189.426	181.6827913	191.6892244	222.4674301
224.3336	184.7468	183.8084195	196.6794877	223.5706016

Figure B.4: Nerja Caves (2011) - Trendline Time Series

Linear Error	Polynomial Error	Power Error	Exponential Error	Logarithmic Error
11.51513333	16.37733333	81.10540503	81.24084138	15.1414919
12.4442	12.9094	78.84842717	81.85251433	12.95406923
12.8316	9.2994	76.42593747	81.85926036	10.84168555
13.05233333	5.922333333	74.14844749	81.63443262	9.049101092
11.93973333	1.611533333	70.8010854	80.0096747	6.316754451
12.28546667	-0.841333333	69.13839735	79.77491955	5.367722261
10.17286667	-5.352933333	65.21443266	77.01172164	2.233249828
5.0186	-12.5066	58.42228826	71.13492248	-3.710485028
6.19766667	-12.92733333	58.11767027	71.51764939	-3.120579208
7.251733333	-13.07346667	57.82622178	71.6996476	-2.48124103
6.09746667	-15.02833333	55.45113454	69.59561232	-3.896967887
6.85986667	-14.66693333	55.10595254	69.32852079	-3.260291373
6.413933333	-15.11426667	53.65584215	67.77129757	-3.710897091
5.051333333	-16.07866667	51.38395658	65.21347985	-4.969542499
4.438733333	-15.89346667	49.94953559	63.31954942	-5.380165328
4.6178	-14.517	49.38772218	62.12893114	-4.910222474
7.0052	-10.5326	51.10941707	63.05599155	-2.150953496
4.18426667	-11.35693333	47.6928286	58.68170397	-4.52592133
-1.01166667	-14.15666667	41.96671127	51.83698025	-9.207843969
-1.665933333	-12.01513333	40.8436216	49.43600258	-9.285393762
-7.778533333	-14.93233333	34.31985411	41.47622178	-14.76330501
-15.0578	-18.6166	26.68372142	32.24668897	-21.35412862
-16.9204	-16.4846	24.51550968	28.32805386	-22.4783047
-17.658	-12.828	23.5207743	25.42589628	-22.43088947
Mean	Mean	Mean	Mean	Mean
3.6369	-8.3668	53.98478727	63.56685477	-3.322210748

Figure B.5: Nerja Caves (2011) - Mean Errors

Linear Absolute Error	Polynomial Absolute Error	Power Absolute Error	Exponential Absolute Error	Logarithmic Absolute Error
11.51513333	16.37733333	81.10540503	81.24084138	15.1414919
12.4442	12.9094	78.84842717	81.85251433	12.95406923
12.8316	9.2994	76.42593747	81.85926036	10.84168555
13.05233333	5.922333333	74.14844749	81.63443262	9.049101092
11.93973333	1.611533333	70.8010854	80.0096747	6.316754451
12.28546667	0.841333333	69.13839735	79.77491955	5.367722261
10.17286667	5.352933333	65.21443266	77.01172164	2.233249828
5.0186	12.5066	58.42228826	71.13492248	3.710485028
6.19766667	12.92733333	58.11767027	71.51764939	3.120579208
7.251733333	13.07346667	57.82622178	71.6996476	2.48124103
6.09746667	15.02833333	55.45113454	69.59561232	3.896967887
6.85986667	14.66693333	55.10595254	69.32852079	3.260291373
6.413933333	15.11426667	53.65584215	67.77129757	3.710897091
5.051333333	16.07866667	51.38395658	65.21347985	4.969542499
4.438733333	15.89346667	49.94953559	63.31954942	5.380165328
4.6178	14.517	49.38772218	62.12893114	4.910222474
7.0052	10.5326	51.10941707	63.05599155	2.150953496
4.18426667	11.35693333	47.6928286	58.68170397	4.52592133
1.01166667	14.15666667	41.96671127	51.83698025	9.207843969
1.665933333	12.01513333	40.8436216	49.43600258	9.285393762
7.778533333	14.93233333	34.31985411	41.47622178	14.76330501
15.0578	18.6166	26.68372142	32.24668897	21.35412862
16.9204	16.4846	24.51550968	28.32805386	22.4783047
17.658	12.828	23.5207743	25.42589628	22.43088947
Mean	Mean	Mean	Mean	Mean
8.644594444	12.21013333	53.98478727	63.56685477	8.480883607

Figure B.6: Nerja Caves (2011) - Absolute Mean Errors

Linear Squared Error	Polynomial Squared Error	Power Squared Error	Exponential Squared Error	Logarithmic Squared Error
132.5982957	268.2170471	6578.086725	6600.074308	229.2647768
154.8581136	166.6526084	6217.074467	6699.834102	167.8079096
164.6499586	86.47884036	5840.923918	6700.938507	117.5421456
170.3634054	35.07403211	5497.992265	6664.180589	81.88623057
142.5572321	2.597039684	5012.793693	6401.548045	39.90138679
150.9326912	0.707841778	4780.117989	6364.037789	28.81244227
103.4872162	28.65389527	4252.922227	5930.80527	4.987404796
25.18634596	156.4150436	3413.163765	5060.177196	13.76769914
38.41107211	167.1159471	3377.663598	5114.774174	9.738014596
52.58763634	170.9155307	3343.871925	5140.839465	6.156557047
37.17909975	225.8508028	3074.828321	4843.549255	15.18635871
47.05777068	215.1189334	3036.666006	4806.443795	10.62949983
41.1385408	228.4410569	2878.949397	4592.948774	13.77075722
25.51596844	258.5235218	2640.310994	4252.797955	24.69635265
19.7023536	252.6022827	2494.956106	4009.365338	28.94617896
21.32407684	210.743289	2439.147102	3860.004085	24.11028474
49.07282704	110.9356628	2612.172513	3976.058071	4.626600941
17.50808754	128.9799347	2274.6059	3443.54238	20.48396388
1.023469444	200.4112111	1761.204855	2687.072522	84.78439055
2.775333871	144.363429	1668.201426	2443.918351	86.21853732
60.50558082	222.9745788	1177.852386	1720.276973	217.9551747
226.7373408	346.5777956	712.0209899	1039.84895	455.9988091
286.2999362	271.7420372	601.0102151	802.4786354	505.2741823
311.804964	164.557584	553.2268239	646.4762018	503.1448022
Mean	Mean	Mean	Mean	Mean
9.753796947	13.01385471	56.3618383	65.76536282	10.5981336

Figure B.7: Nerja Caves (2011) - Mean Squared Errors

Linear Absolute Squared Error	Polynomial Absolute Squared Error	Power Absolute Squared Error	Exponential Absolute Squared Error	Logarithmic Absolute Squared Error
132.5982957	268.2170471	6578.086725	6600.074308	229.2647768
154.8581136	166.6526084	6217.074467	6699.834102	167.8079096
164.6499586	86.47884036	5840.923918	6700.938507	117.5421456
170.3634054	35.07403211	5497.992265	6664.180589	81.88623057
142.5572321	2.597039684	5012.793693	6401.548045	39.90138679
150.9326912	0.707841778	4780.117989	6364.037789	28.81244227
103.4872162	28.65389527	4252.922227	5930.80527	4.987404796
25.18634596	156.4150436	3413.163765	5060.177196	13.76769914
38.41107211	167.1159471	3377.663598	5114.774174	9.738014596
52.58763634	170.9155307	3343.871925	5140.839465	6.156557047
37.17909975	225.8508028	3074.828321	4843.549255	15.18635871
47.05777068	215.1189334	3036.666006	4806.443795	10.62949983
41.1385408	228.4410569	2878.949397	4592.948774	13.77075722
25.51596844	258.5235218	2640.310994	4252.797955	24.69635265
19.7023536	252.6022827	2494.956106	4009.365338	28.94617896
21.32407684	210.743289	2439.147102	3860.004085	24.11028474
49.07282704	110.9356628	2612.172513	3976.058071	4.626600941
17.50808754	128.9799347	2274.6059	3443.54238	20.48396388
1.023469444	200.4112111	1761.204855	2687.072522	84.78439055
2.775333871	144.363429	1668.201426	2443.918351	86.21853732
60.50558082	222.9745788	1177.852386	1720.276973	217.9551747
226.7373408	346.5777956	712.0209899	1039.84895	455.9988091
286.2999362	271.7420372	601.0102151	802.4786354	505.2741823
311.804964	164.557584	553.2268239	646.4762018	503.1448022
Mean	Mean	Mean	Mean	Mean
95.13655488	169.3604144	3176.658817	4325.082947	112.3204358
Mean Square Root	Mean Square Root	Mean Square Root	Mean Square Root	Mean Square Root
9.753796947	13.01385471	56.3618383	65.76536282	10.5981336

Figure B.8: Nerja Caves (2011) - Absolute Mean Squared Errors

Month	Radon Concentration	12 Period Centred MA	Monthly Variation
7	488	174.5833333	313.4166667
8	436	177.625	258.375
9	365	180.125	184.875
10	173	182.4583333	-9.458333333
11	34	183.4583333	-149.4583333
12	29	185.9166667	-156.9166667
13	67	185.9166667	-118.9166667
14	62	182.875	-120.875
15	67	186.1666667	-119.1666667
16	75	189.3333333	-114.3333333
17	86	190.2916667	-104.2916667
18	381	193.1666667	187.8333333
19	424	194.8333333	229.1666667
20	427	195.5833333	231.4166667
21	453	197.0833333	255.9166667
22	161	199.375	-38.375
23	69	203.875	-134.875
24	63	203.1666667	-140.1666667
25	73	200.0833333	-127.0833333
26	74	201.5416667	-127.5416667
27	91	197.5416667	-106.5416667
28	106	192.375	-86.375
29	163	192.625	-29.625
30	287	194	93

Figure B.9: Nerja Caves (2011) - Monthly Variation in Radon Concentration

Month	Linear	Seasonal Averages	Seasonal Forecast
1	150.3926	-120.0208333	30.37176667
2	152.5052	-120.0208333	32.48436667
3	154.6178	-120.0208333	34.59696667
4	156.7304	-8.965277778	147.7651222
5	158.843	-8.965277778	149.8777222
6	160.9556	-8.965277778	151.9903222
7	163.0682	245.5277778	408.5959778
8	165.1808	245.5277778	410.7085778
9	167.2934	245.5277778	412.8211778
10	169.406	-104.875	64.531
11	171.5186	-104.875	66.6436
12	173.6312	-104.875	68.7562
13	175.7438	-120.0208333	55.72296667
14	177.8564	-120.0208333	57.83556667
15	179.969	-120.0208333	59.94816667
16	182.0816	-8.965277778	173.1163222
17	184.1942	-8.965277778	175.2289222
18	186.3068	-8.965277778	177.3415222
19	188.4194	245.5277778	433.9471778
20	190.532	245.5277778	436.0597778
21	192.6446	245.5277778	438.1723778
22	194.7572	-104.875	89.8822
23	196.8698	-104.875	91.9948
24	198.9824	-104.875	94.1074
25	201.095	-120.0208333	81.07416667
26	203.2076	-120.0208333	83.18676667
27	205.3202	-120.0208333	85.29936667
28	207.4328	-8.965277778	198.4675222
29	209.5454	-8.965277778	200.5801222
30	211.658	-8.965277778	202.6927222
31	213.7706	245.5277778	459.2983778
32	215.8832	245.5277778	461.4109778
33	217.9958	245.5277778	463.5235778
34	220.1084	-104.875	115.2334
35	222.221	-104.875	117.346
36	224.3336	-104.875	119.4586

Figure B.10: Nerja Caves (2011) - Seasonal Variation Forecast Model

Month	Linear	Monthly Averages	Monthly Forecast
1	150.3926	-123	27.3926
2	152.5052	-124.2083333	28.29686667
3	154.6178	-112.8541667	41.76363333
4	156.7304	-100.3541667	56.37623333
5	158.843	-66.95833333	91.88466667
6	160.9556	140.4166667	301.3722667
7	163.0682	271.2916667	434.3598667
8	165.1808	244.8958333	410.0766333
9	167.2934	220.3958333	387.6892333
10	169.406	-23.91666667	145.4893333
11	171.5186	-142.1666667	29.35193333
12	173.6312	-148.5416667	25.08953333
13	175.7438	-123	52.7438
14	177.8564	-124.2083333	53.64806667
15	179.969	-112.8541667	67.11483333
16	182.0816	-100.3541667	81.72743333
17	184.1942	-66.95833333	117.2358667
18	186.3068	140.4166667	326.7234667
19	188.4194	271.2916667	459.7110667
20	190.532	244.8958333	435.4278333
21	192.6446	220.3958333	413.0404333
22	194.7572	-23.91666667	170.8405333
23	196.8698	-142.1666667	54.70313333
24	198.9824	-148.5416667	50.44073333
25	201.095	-123	78.095
26	203.2076	-124.2083333	78.9926667
27	205.3202	-112.8541667	92.46603333
28	207.4328	-100.3541667	107.0786333
29	209.5454	-66.95833333	142.5870667
30	211.658	140.4166667	352.0746667
31	213.7706	271.2916667	485.0622667
32	215.8832	244.8958333	460.7790333
33	217.9958	220.3958333	438.3916333
34	220.1084	-23.91666667	196.1917333
35	222.221	-142.1666667	80.05433333
36	224.3336	-148.5416667	75.79193333

Figure B.11: Nerja Caves (2011) - Monthly Variation Forecast Model

Error (Seasonal Forecast)	Error (Monthly Forecast)	Squared Error (Seasonal Forecast)	Squared Error (Monthly Forecast)
-3.371766667	-0.3926	11.36881045	0.15413476
-3.484366667	0.703133333	12.14081107	0.494396484
5.403033333	-1.763633333	29.1927692	3.110402534
-101.7651222	-10.37623333	10356.1401	107.6662182
-58.87772222	-0.884666667	3466.586174	0.782635111
165.0096778	15.62773333	27228.19376	244.2260491
79.40402222	53.64013333	6304.998745	2877.263904
25.29142222	25.92336667	639.656038	672.0209393
-47.82117778	-22.68923333	2286.865044	514.8013093
108.469	27.51066667	11765.52396	756.8367804
-32.6436	4.648066667	1065.604621	21.60452374
-39.7562	3.910466667	1580.555438	15.29174955
11.27703333	14.2562	127.1714808	203.2392384
4.164433333	8.351933333	17.34250499	69.7547904
7.051833333	-0.114833333	49.72835336	0.013186694
-98.11632222	-6.727433333	9626.812686	45.25835925
-89.22892222	-31.23586667	7961.800561	975.6793664
203.6584778	54.27653333	41476.77557	2945.942071
-9.947177778	-35.71106667	96.94634574	1275.280282
-9.059777778	-8.427833333	82.07957338	71.02837469
14.82762222	39.95956667	219.9593808	1596.766368
71.1178	-9.840533333	5057.741477	96.83509628
-22.9848	14.29686667	528.760827	204.4003965
-31.1074	12.55926667	967.6703348	157.7351792
-8.074166667	-5.095	65.19216736	25.959025
-9.186766667	-4.999266667	84.39668179	24.992672
5.700633333	-1.466033333	32.4972204	2.149253734
-92.46752222	-1.078633333	8550.242666	1.163449868
-37.58012222	20.41293333	1412.265586	416.6878473
84.30727778	-65.07466667	7107.717086	4234.712242
-15.29837778	-41.06226667	234.0403626	1686.109744
-19.41097778	-18.77903333	376.7860583	352.6520929
-121.5235778	-96.39163333	14767.97996	9291.346977
32.7666	-48.19173333	1073.650076	2322.443162
-29.346	7.945666667	861.187716	63.13361878
-42.4586	1.208066667	1802.732714	1.459425071
Mean	Mean	Mean	Mean
-2.918655556	-2.918655556	4648.061185	868.8610238
		Square Root	Square Root
		68.17669092	29.47644863

Figure B.12: Nerja Caves (2011) - Forecast Model Error Results

Month	Radon Concentration (Bq/m3)	Monthly Variations	Linear Trendline	Forecast	Error	Squared Error
1	65	-123	150.3926	27.3926	37.6074	1414.316535
2	60	-124.2083333	152.5052	28.29686667	31.70313333	1005.088663
3	65	-112.8541667	154.6178	41.76363333	23.23636667	539.9287359
4	72	-100.3541667	156.7304	56.37623333	15.62376667	244.1020849
5	80	-66.96833333	158.843	91.88466667	-11.88466667	141.2453018
6	368	140.4166667	160.9556	301.3722667	66.62773333	4439.254849
7	422	271.2916667	163.0682	434.3598667	-12.35986667	152.766304
8	425	244.8958333	165.1808	410.0766333	14.92336667	222.7068727
9	450	220.3958333	167.2934	387.6892333	62.31076667	3882.631643
10	135	-23.91666667	169.406	145.4893333	-10.48933333	110.0261138
11	66	-142.1666667	171.5186	29.35193333	36.64806667	1343.08079
12	61	-148.5416667	173.6312	25.08953333	35.91046667	1289.561616
					Mean	Mean
					24.15476667	1232.059126
						Square Root
						35.10069979

Figure B.13: Nerja Caves (2005) - Forecast Model Error Results

# Appendix C

## Symbols

The symbols in the following table are shown in the order they appear in the text.

Symbol	Description
E	Effective dose
$C_{Rn}$	Radon concentration
t	Time
DCF	Dose Conversion Factor
F	Equilibrium factor
PAEC	Potential alpha energy concentration
D	Dose rate in air 1m above the ground
$C_{Ra}$	Radium concentration
$C_{Th}$	Thorium concentration
$C_K$	Potassium concentration
a, b, c	Constants
$\frac{dC}{dt}$	Rate of change of radon concentration with time
S	Surface area
V	Volume
$\Phi$	Radon flux
$\lambda$	Radioactivity decay constant for radon
$\lambda_V$	Ventilation rate
$C_{ext}$	Outside radon concentration
$\bar{C}$	Steady state radon concentration with ventilation
$\bar{C}$	Steady state radon concentration without ventilation
$\lambda_V^{winter}$	Winter ventilation flow rate
$C_{summer}$	Summer radon concentration
$C_{winter}$	Winter radon concentration
$Q_V$	Volumetric flow rate
$V_{tot}$	Total volume of quarry
$C_{cave}$	Radon concentration in cave
$C_{out}$	Radon concentration outside cave
$k_i$	Temperature related constant
$\Delta T$	Difference between outside and cave temperature
L	Distance of measurement point from cave entrance
$C_n, C_{n+1}$	Radon concentrations on two consecutive days
h	Height of accumulation chamber
$\Delta C_{Rn}$	Difference in radon concentration inside and outside accumulation chamber
$\Delta t$	Accumulation period
$E_M$	Emanation coefficient
$V_C$	Volume of measurement chamber
$V_S$	Volume of sample
$\rho$	Density of sample
$V_{cyl}$	Volume of container
$S_{cyl}$	Base surface area of container
$T_{acc}$	Accumulation time 63
$z^*$	Diffusion length of radon in rock

# Appendix D

## Glossary

**Absorbed dose** - Energy deposition in any medium by any type of ionizing radiation [20].

**Becquerel, Bq** - The SI unit of radioactivity, one nuclear disintegration per second.

**Dose Conversion Factor (DCF)** - A number of mSv per WLM, varies according to circumstances, location etc..

**Effective dose** - An indicator of the effects of radiation on the body as a whole when different body tissues are exposed to different levels of equivalent dose [20].

**Equilibrium factor** - The level of equilibrium of radon with its daughter products (radionuclides further down its decay chain.)

**Equivalent dose** - A measure of the biological effect of radiation, the unit is the Sievert. Equivalent Dose = Absorbed Dose x Radiation Weighting Factor [20].

**Radiation Weighting Factor,  $W_R$**  - The measure of the ability of a particular type of radiation to cause biological damage [20].

**Sievert, Sv** - The unit of equivalent dose [20]. Often shown as  $\mu Sv$  or mSv.

**Unattached fraction** - The fraction of a radionuclide not attached to aerosols in the atmosphere.

**Working Level Month (WLM)** - 1 WLM is 170 hours exposure to a radon daughter product concentration of  $21 \mu Jm^{-3}$  potential  $\alpha$ -energy [34].

# Bibliography

- [1] Allodji, R. S., Leuraud, K., Bernhard, S., Henry, S., Bénichou, J., Laurier, D.. Assessment of uncertainty associated with measuring exposure to radon and decay products in the French uranium miners cohort. *Journal of Radiological Protection* 32 (2012) 85-100.
- [2] Cevik, U., Kara, A., Celik, N., Karabidak, M., Celik, A.. Radon Survey and Exposure Assessment in Karaca and Çal Caves, Turkey. *Water Air Soil Pollut* (2011) 214:461-469.
- [3] Denman, A. R., Parkinson, S.. Estimates of radiation dose to National Health Service workers in Northamptonshire from raised radon levels: Short communication. *British Journal of Radiology* 69 (1996) 72-75.
- [4] Dueñas, C., Fernández, M. C., Cañete, S., Carretero, J., Liger, E..  $^{222}\text{Rn}$  concentrations, natural flow rate and the radiation exposure levels in the Nerja Cave. *Atmospheric Environment* 33 (1999) 501-510.
- [5] Dueñas, C., Fernández, M. C., Cañete, S..  $^{222}\text{Rn}$  concentrations and the radiation exposure levels in the Nerja Cave. *Radiation Measurements* 40 (2005) 630-632.
- [6] Dueñas, C., Fernández, M. C., Cañete, S., Pérez, M., Gordo, E.. Seasonal variations of radon and the radiation exposure levels in Nerja Cave, Spain. *Radiation Measurements* 46 (2011) 1181-1186.
- [7] Espinosa, G., Golzarri, J. I., Gammage, R. B., Sajo-Bohus, L., Viccon-Pale, J., Signoret-Poillon, M.. Seasonal variation measurements of radon levels in caves using SSNTD method. *Radiation Measurements* 43 (2008) S364-S368.
- [8] European Commission. Council Directive 96/29/EURATOM of 13 May 1996 laying down basic safety standards for the protection of the health of workers and the general public against the dangers arising from ionising radiation. *Off. J. Eur. Commun.*, L159 (1996).

- [9] Garavaglia, M., Braitenberg, C., Zadro, M. Radon Monitoring in a Cave of North-Eastern Italy. *Phys. Chem. Earth*, Vol. 23, No. 9-10, pp. 949-952, 1998.
- [10] Géczy, G., Hunyadi, I., Hakl, J.. Long term radon studies and transport processes in the Budapest thermal karst region. *Bulletin de la Société géologique de Liège*, 29, 1993, 45-48.
- [11] Gillmore, G. K., Phillips, P. S., Denman, A. R., Gilbertson, D. D.. Radon in the Creswell Crags Permian limestone caves. *Journal of Environmental Radioactivity* 62 (2002) 165-179.
- [12] Grattan, J. P., Gillmore, G. K., Gilbertson, D. D., Pyatt, F. B., Hunt, C. O., McLaren, S. J., Phillips, P. S., Denman, A.. Radon and “King Solomon’s Miners”: Faynan Orefield, Jordanian Desert. Aberystwyth University, Cadair Online Research Repository (<http://cadair.aber.ac.uk/dspace/>).
- [13] Gregorič, A., Zidanšek, A., Vaupotič, J.. Dependence of radon levels in Postojna Cave on outside air temperature. *Nat. Hazards Earth Syst.*, 11,1523-1528, 2011.
- [14] Hafez, A. F., Hussein, A. S.. Radon activity concentrations and effective doses in ancient Egyptian tombs of the Valley of the Kings. *Applied Radiation and Isotopes* 55 (2001) 355-362.
- [15] Ionising Radiations Regulations (1999). Health and Safety Executive, Statutory Instrument 3232, HMSO.
- [16] Kant, K., Kuriakose, S., Sharma, G. S.. Radon activity and the radiation dose levels in the slate mines in aravali range in India. *Journal of Geology and Mining Research* Vol. 1(7)pp. 156-158, September, 2009.
- [17] Koltai, G., Ország, J., Tegzes, Z., Bárány-Kevei, I. Radon transport measurements in Mecsek Mountains. *Acta Carsologica* 39/3, 513-522, Postojna 2010.
- [18] Kowalczyk, A. J., Freolich, P. N.. Cave air ventilation and  $CO_2$  outgassing by radon-222 modeling: How fast do caves breathe? *Earth and Planetary Science Letters* 289 (2010) 209-219.
- [19] Lario, J., Sánchez-Moral, S., Cañaveras, J. C., Cuezva, S., Soler, V.. Radon continuous monitoring in Altamira Cave (northern Spain) to assess user’s annual effective dose. *Journal of Environmental Radioactivity* 80 (2005) 161-174.

- [20] Martin, A., Harbison, S. A.. An Introduction to Radiation Protection - Fourth Edition. Arnold, London, 1996. ISBN 0-412-63110-5.
- [21] Radiation Protection Training Course Notes: Public Exposure - Radon. UK National Radiation Protection Board.
- [22] Perrier, F., Richon, P., Crouzeix, C., Morat, P., Le Mouël, J-L.. Radon-222 signatures of natural ventilation regimes in an underground quarry. *Journal of Environmental Radioactivity* 71 (2004) 17-32.
- [23] Perrier, F., Richon, P., Sabroux, J-C.. Modelling the affect of air exchange on  $^{222}\text{Rn}$  and its progeny concentration in a tunnel atmosphere. *Science of the Total Environment* 350 (2005) 136-150.
- [24] Perrier, F., Richon, P., Gautam, U., Tiwari, D. R., Shrestha, P., Sapkota, S. N.. Seasonal variations of natural ventilation and radon-222 exhalation in a slightly rising dead-end tunnel. *Journal of Environmental Radioactivity* 97 (2007) 220-235.
- [25] Przylibski, T. A.. Radon concentration changes in the air of two caves in Poland. *Journal of Environmental Radioactivity* 45 (1999) 81-94.
- [26] Qureshi, A. A., Kakar, D. M., Akram, M., Khattak, N. U., Tufail, M., Mehmood, K., Jamil, K., Khan, H. A.. Radon concentrations in coal mines of Baluchistan, Pakistan. *Journal of Environmental Radioactivity* 48 (2), 203-209, (2000).
- [27] Richon, P., Perrier, F., Sabroux, J-C., Trique, M., Ferry, C., Voisin, V., Pili, E.. Spatial and time variations of radon-222 concentrations in the atmosphere of a dead-end horizontal tunnel. *Journal of Environmental Radioactivity* 78 (2005) 179-198.
- [28] Sainz, C., Quindós, L., S., Fuente, I., Nicolás, J., Quindós, L.. Analysis of the main factors affecting the evaluation of the radon dose in workplaces: the case of tourist caves. *Journal of Hazardous Materials* 145 (2007) 368-371.
- [29] Smetanova, I., Holý, K., Jurčák, D., Omelka, J., Zelinka, J.. Radon monitoring in Domic Cave, Slovakia - A preliminary Results. 6th ISCA Congress Proceedings (2011) pp. 136-140. ISBN 978-80-89310-59-3.
- [30] Tanahara, A., Taria, H., Takemura, M.. Radon distribution and the ventilation of a limestone cave on Okinawa. *Geochemical Journal*, Vol. 31, pp. 49 to 56, 1997.

- [31] Tsvetkova, T., Przylibski, T. A., Nevinsky, I., Nevinsky, V.. Measurement of radon in the East Europe under the ground. *Radiation Measurements* 40 (2005) 98-105.
- [32] Vaupotič, J.. Radon levels in karst caves in Slovenia. *Acta Carsologica* 39/3, 503-512, Postojna 2010.
- [33] Wilkening, M. H., Watkins, D. E.. Air exchange and Rn-222 in the Carlsbad Caverns. *Health Physics*, 31, 139-145, 1976.
- [34] Zahorowski, W., Whittlestone, S., James, J., Solomon, S.. Radon in a tourist cave: A one year continuous survey of the concentrations of attached and unattached radon progeny and radon. *Radon in the Living Environment*, 19-23 April 1999, Athens, Greece.